Polarized emission from strongly magnetized sources

Roberto Taverna

Dipartimento di Fisica e Astronomia G. Galilei
Università degli Studi di Padova

Dipartimento di Matematica e Fisica
Università degli Studi di Roma Tre

107° Congresso Nazionale – Società Italiana di Fisica
13 – 17 Settembre 2021

Introduction

- **Roberto Taverna**
  Researcher at Department of Astronomy and Astrophysics «G. Galilei»
  University of Padova

- In collaboration with Roberto Turolla (dfa-unipd, UCL-MSSL), Silvia Zane (UCL-MSSL), Valery Suleimanov (IAA-Tubingen), Alexander Potekhin (IOFFE-St. Petersburg)

- Email: roberto.taverna@pd.infn.it
  roberto.taverna@unipd.it

Overview

- Theoretical model to simulate spectral and polarization properties of magnetar X-ray emission
- Comparison with the simulated response of forthcoming, new-generation X-ray polarimeters ($IXPE$, $eXTP$)
- Obtaining information on
  - the geometry and physics of the source
  - the physical state of the star surface
  - testing QED vacuum polarization

Neutron star zoo

- Neutron stars (NSs) are relics of massive stars ($M \approx 8 - 25\ M_{\odot}$)
  - masses $M_{\mathrm{NS}} \approx 1 - 2\ M_{\odot}$
  - radii $R_{\mathrm{NS}} \approx 10 - 15$ km
  - spin periods $P \approx 10^{-2} - 10$ s
  - period derivatives $\dot{P} \approx 10^{-20} - 10^{-9}$ s/s
  - strong magnetic fields

$$B_{\mathrm{sd}} \approx 3.2 \times 10^{19}\sqrt{P\dot{P}}\ \mathrm{G} \quad \rightarrow \quad B_{NS} \approx 10^{12}\ \mathrm{G}$$

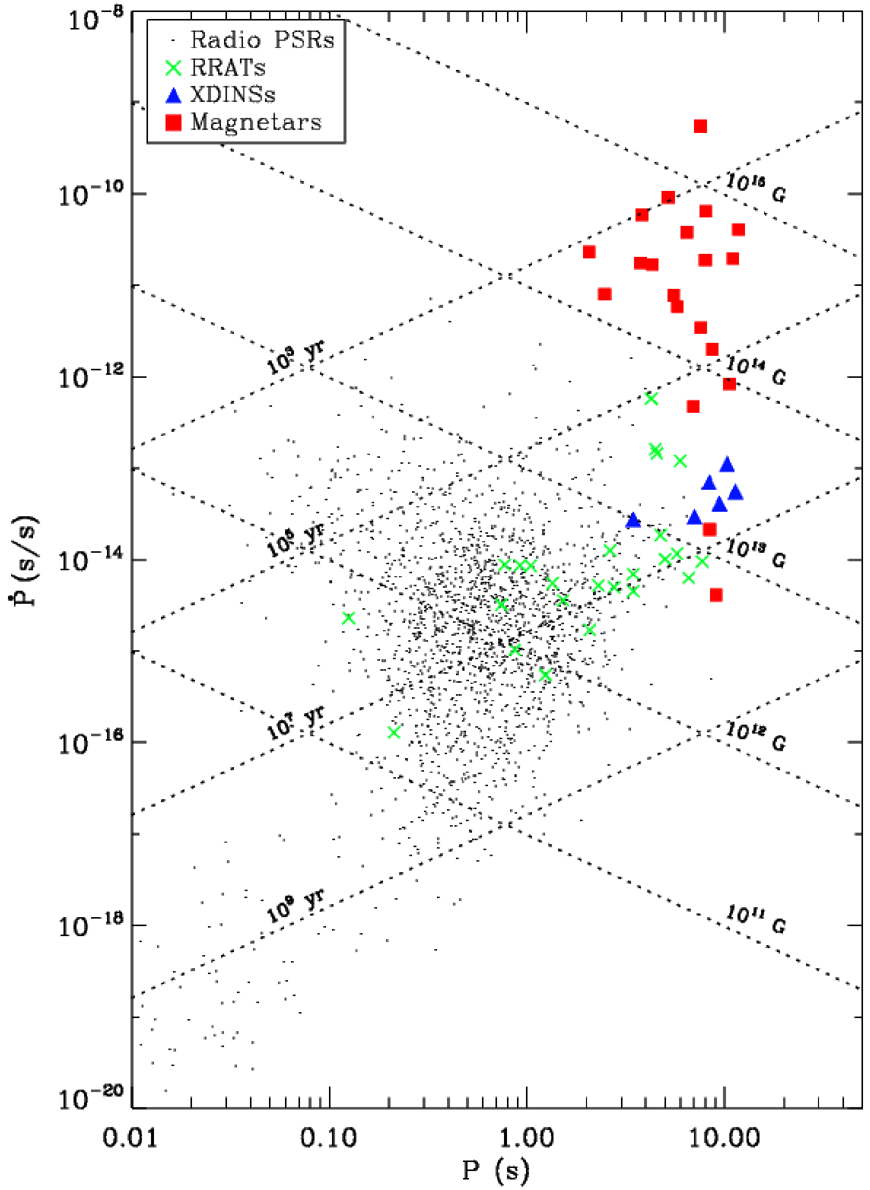

Neutron star zoo

- Neutron stars (NSs) are relics of massive stars ($M \approx 8 - 25\, M_\odot$)
  - masses $M_\mathrm{NS} \approx 1 - 2\, M_\odot$
  - radii $R_\mathrm{NS} \approx 10 - 15$ km
  - spin periods $P \approx 10^{-2} - 10$ s
  - period derivatives $\dot{P} \approx 10^{-20} - 10^{-9}$ s/s
  - strong magnetic fields

$$B_\mathrm{sd} \approx 3.2 \times 10^{19} \sqrt{P\dot{P}}\ \mathrm{G} \quad \rightarrow \quad B_{NS} \approx 10^{12}\ \mathrm{G}$$

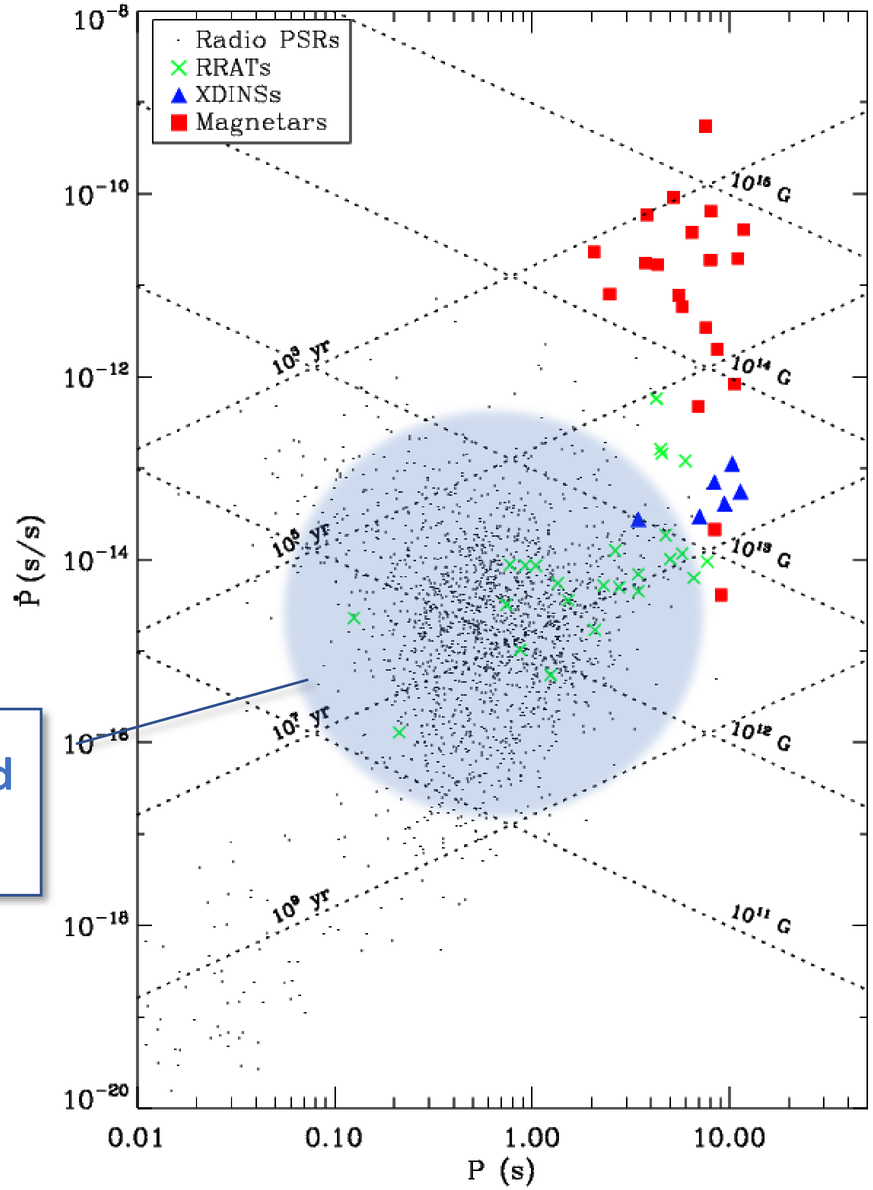

Neutron star zoo

- Neutron stars (NSs) are relics of
  ($M \approx 8 - 25\ M_\odot$)
  - masses $M_{\rm NS} \approx 1 - 2\ M_\odot$
  - radii $R_{\rm NS} \approx 10 - 15$ km
  - spin periods $P \approx 10^{-2} - 10$ s
  - period derivatives $\dot{P} \approx 10^{-20} - 10^{-9}$ s/s
  - strong magnetic fields

$$B_{\rm sd} \approx 3.2 \times 10^{19} \sqrt{P\dot{P}}\ \mathrm{G} \quad \rightarrow \quad B_{NS} \approx 10^{12}\ \mathrm{G}$$

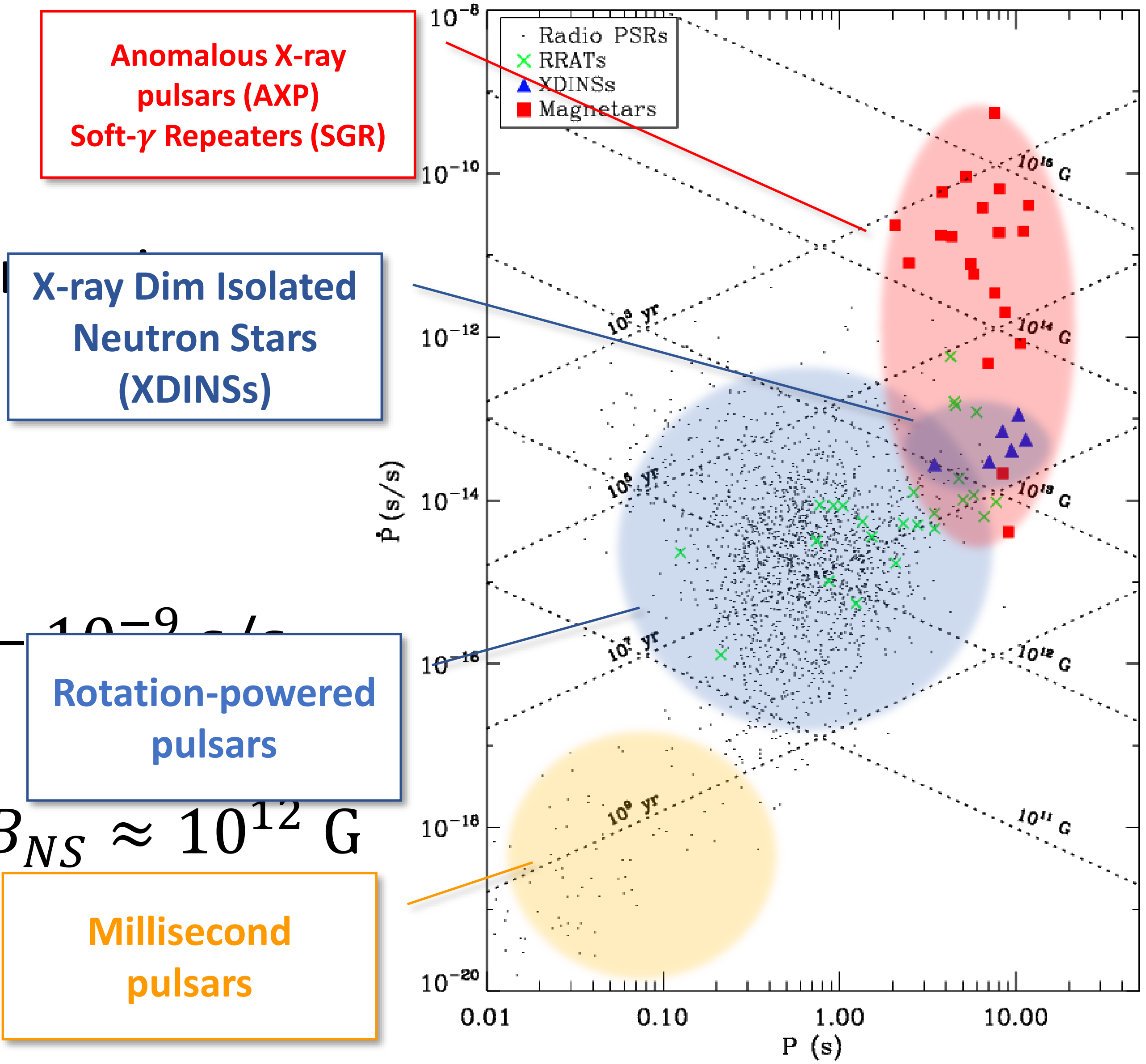

AXPs and SGRs

- Longer spin periods and larger spin-down rates

$$P \approx 2 - 12 \text{ s}$$
$$\dot{P} \approx 10^{-13} - 10^{-9} \text{ s/s}$$
$$\Rightarrow \quad B_{\mathrm{sd}} \approx 10^{14} - 10^{15} \text{ G}$$

Magnetars!

- Radio-silent sources (mostly)

- X-ray luminosity usually exceeding the rotational energy losses

$$L_{\mathrm{X}} > \dot{E}_{\mathrm{rot}} = I\Omega\dot{\Omega}$$

Anomalous!

AXPs and SGRs – Persistent emission

- Soft X-ray spectra ($0.5 - 10$ keV) well fitted by a thermal (BB) component ($T \approx 0.5$ keV) and a power-law ($\Gamma \approx 2 - 4$)

- Purely thermal spectra (BB+BB) tipically for transient sources

- X-ray luminosity $L_X \approx 10^{33} - 10^{36}$ erg/s

- Additional PL component ($\Gamma \approx 1 - 2$) at higher energies ($\gtrsim 20$ keV)

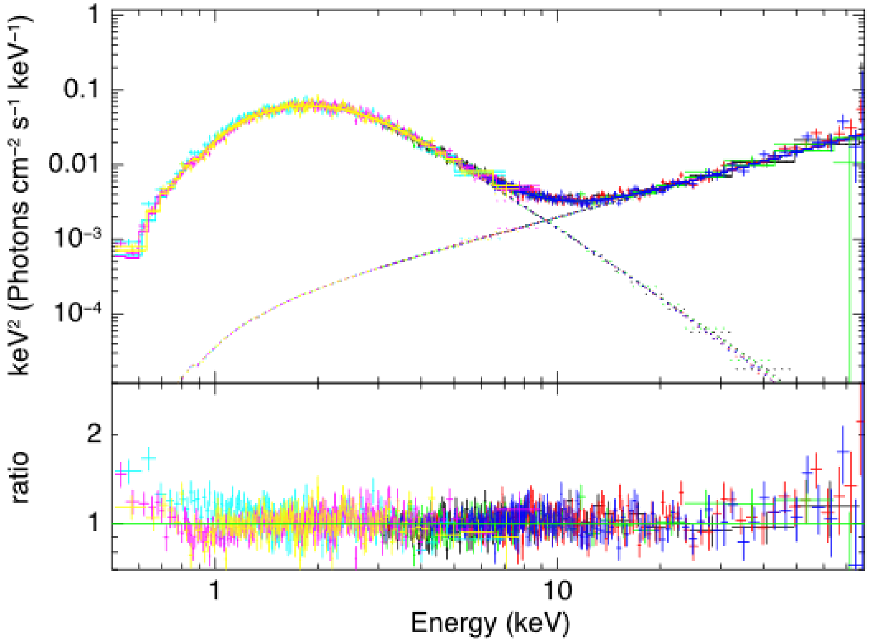

Tendulkar et al. (2015)

AXPs and SGRs – Bursting activity

- Short bursts
  - $\Delta t \approx 0.01 - 1$ s
  - $L_X \approx 10^{36} - 10^{42}$ erg/s
- Intermediate flares
  - $\Delta t \approx 1 - 10$ s
  - $L_X \approx 10^{41} - 10^{43}$ erg/s
- Giant flares
  - $\Delta t \approx 10^2$ s
  - $L_X \approx 10^{44} - 10^{47}$ erg/s

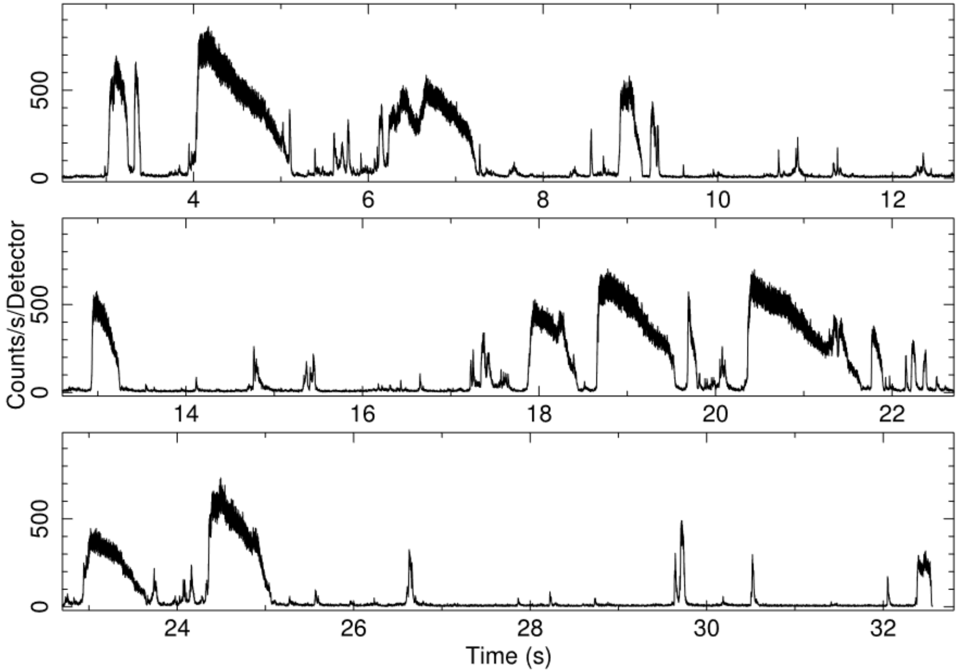

Israel et al. (2008)

Twisted-magnetosphere model

- The internal magnetic field of the star develops a strong toroidal component

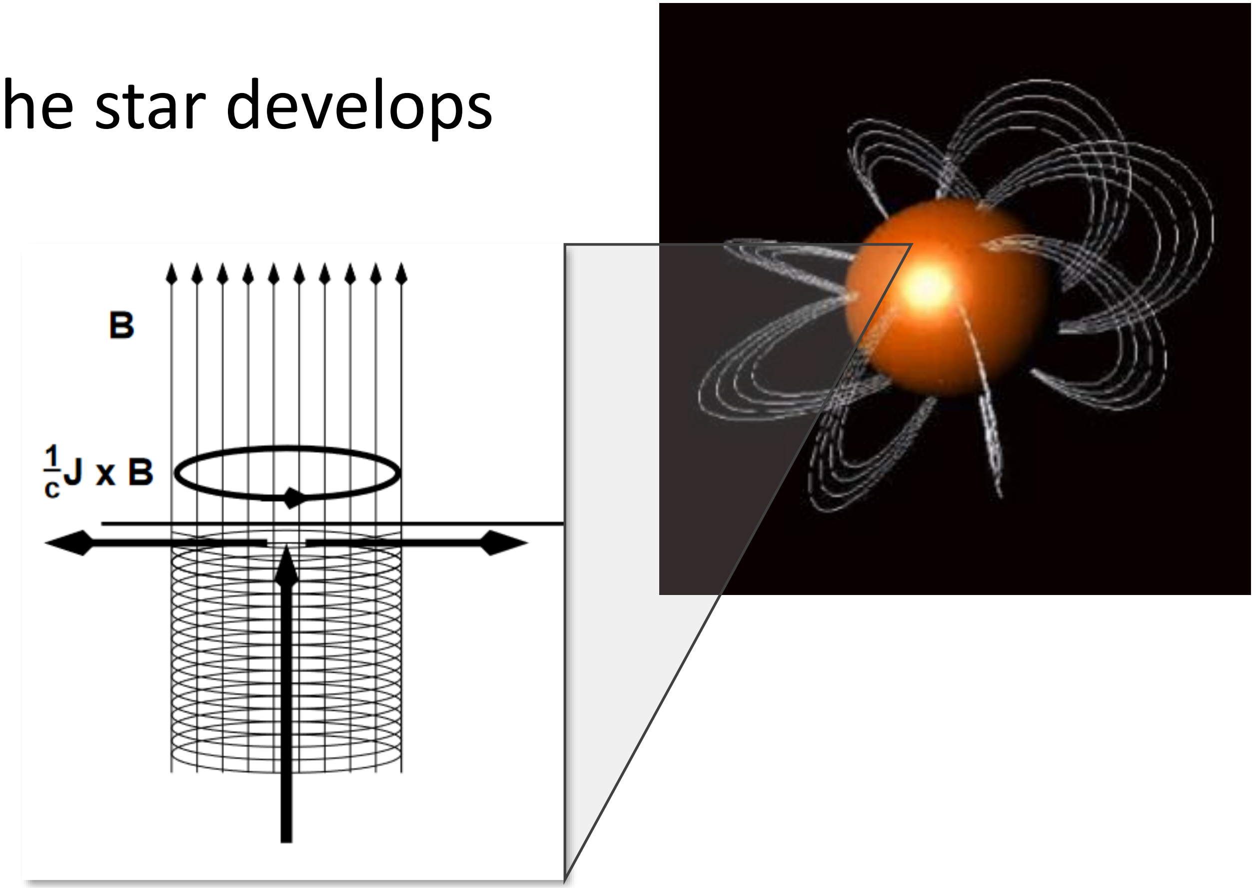

Twisted-magnetosphere model

- The internal magnetic field of the star develops a strong toroidal component
- Once the magnetic stress exceeds the mechanical yield of the crust the external field becomes «twisted»

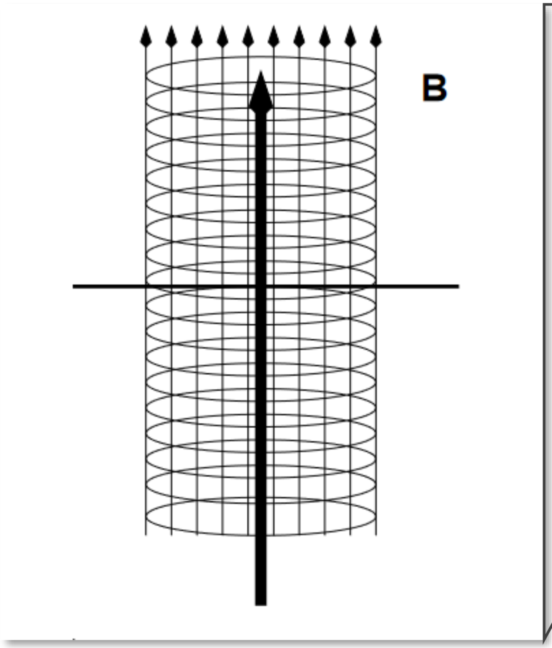

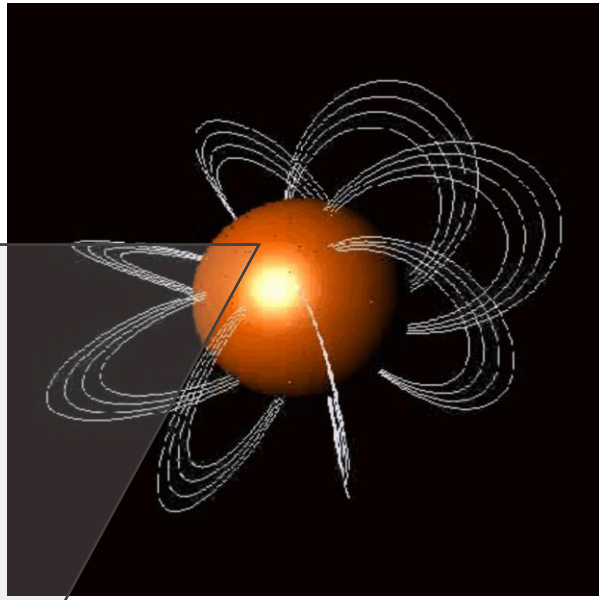

Twisted-magnetosphere model

- The internal magnetic field of the star develops a strong toroidal component
- Once the magnetic stress exceeds the mechanical yield of the crust the external field becomes «twisted»
- Twist angle

$$\Delta\phi_{\mathrm{N-S}} = 2\lim_{\theta\to 0}\int_{\theta}^{\pi/2}\frac{B_{\phi}}{\sin\theta\, B_{\theta}}\,d\theta$$

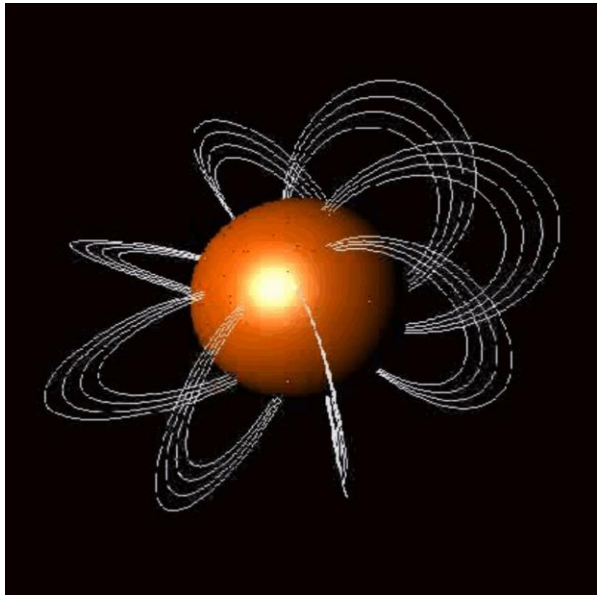

Magnetospheric currents

- Non-potential field ⇒ charged particles must flow along the closed field lines

$$n_e \propto \frac{B}{r\beta}\left(\frac{B_\phi}{B_\theta}\right)$$

- Thermal photons will resonantly scatter onto moving charged particles

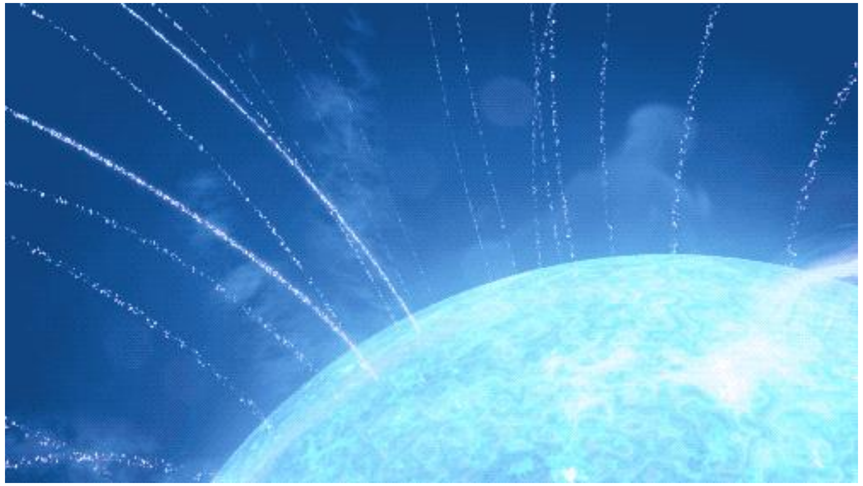

Media INAF

Magnetar model achievements

- Resonant scattering onto magnetospheric particles generates power-law spectral tails in soft X-ray spectra
- Due to crustal deformations caused by the internal field $e^{-}e^{+}$ fireballs are injected in the magnetosphere (generating short burst and giant flare emission)

Polarization in strong B-fields – QED effects

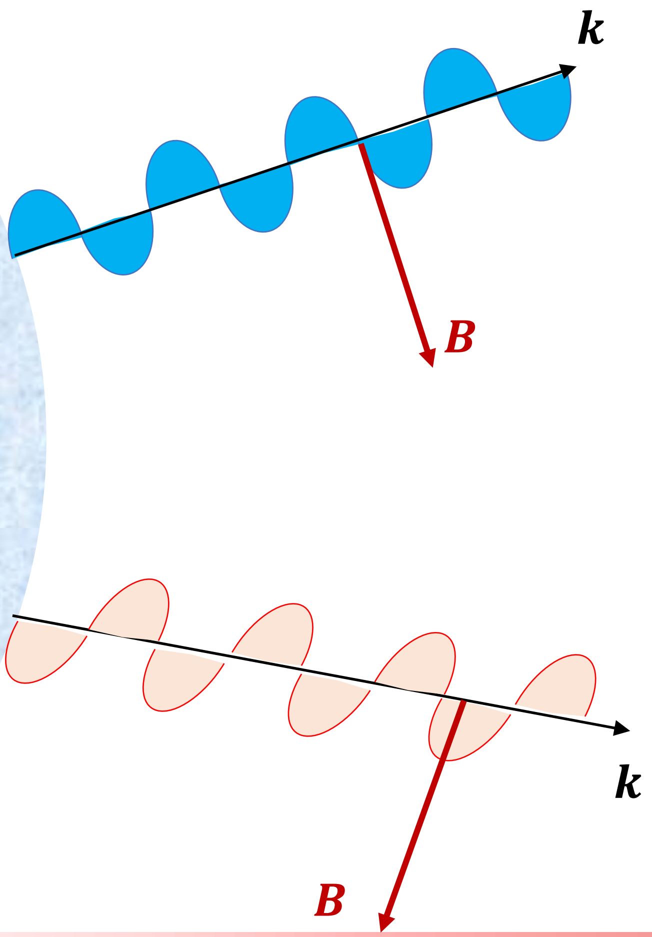

- Photons propagating in the strongly-magnetized vacuum around the star are linearly polarized in two normal modes:
  - O-mode (photon electric field oscillating in the kB plane)
  - X-mode (photon electric field oscillating ortogonally to both $\boldsymbol{k}$ and $\boldsymbol{B}$)

Polarization in strong B-fields – QED effects

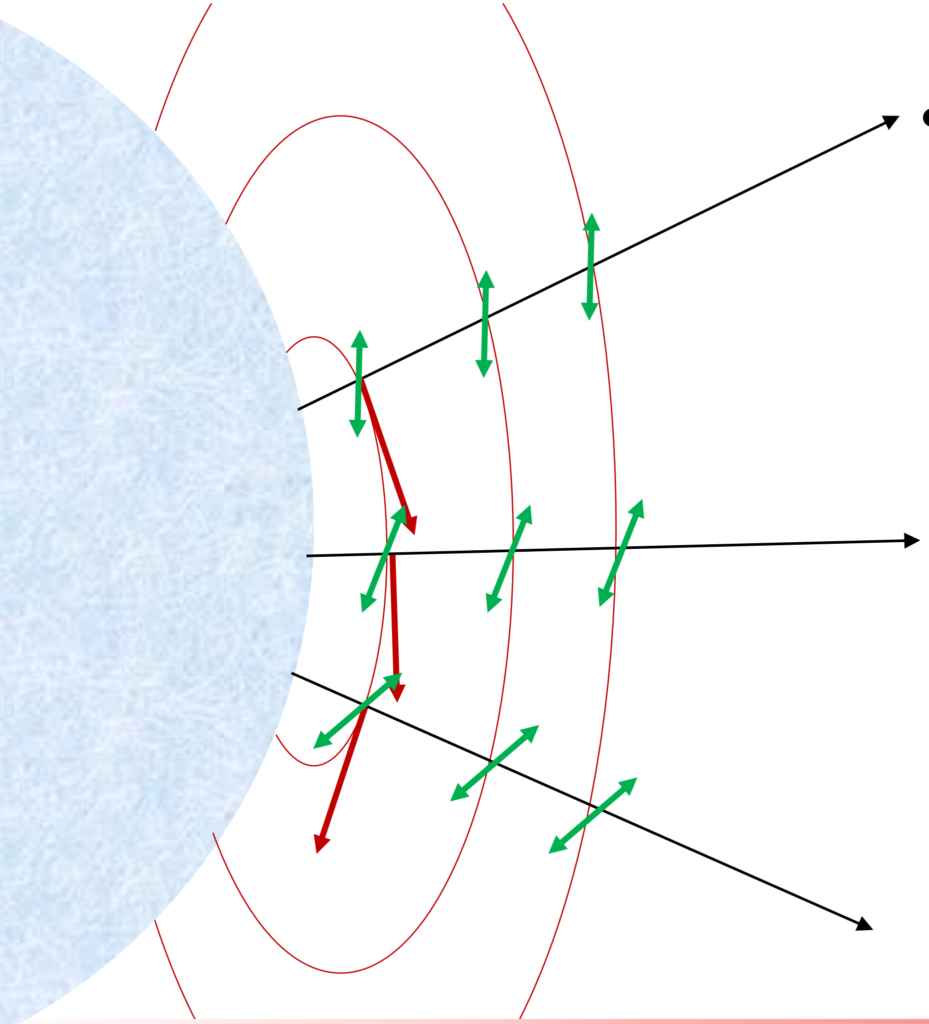

- The polarization pattern of photons at the surface should be quite reduced due to the rapid variation of the magnetic field at the emission

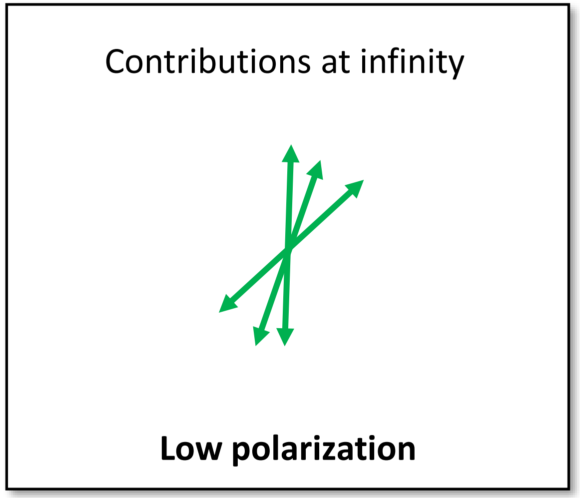

Polarization in strong B-fields – QED effects

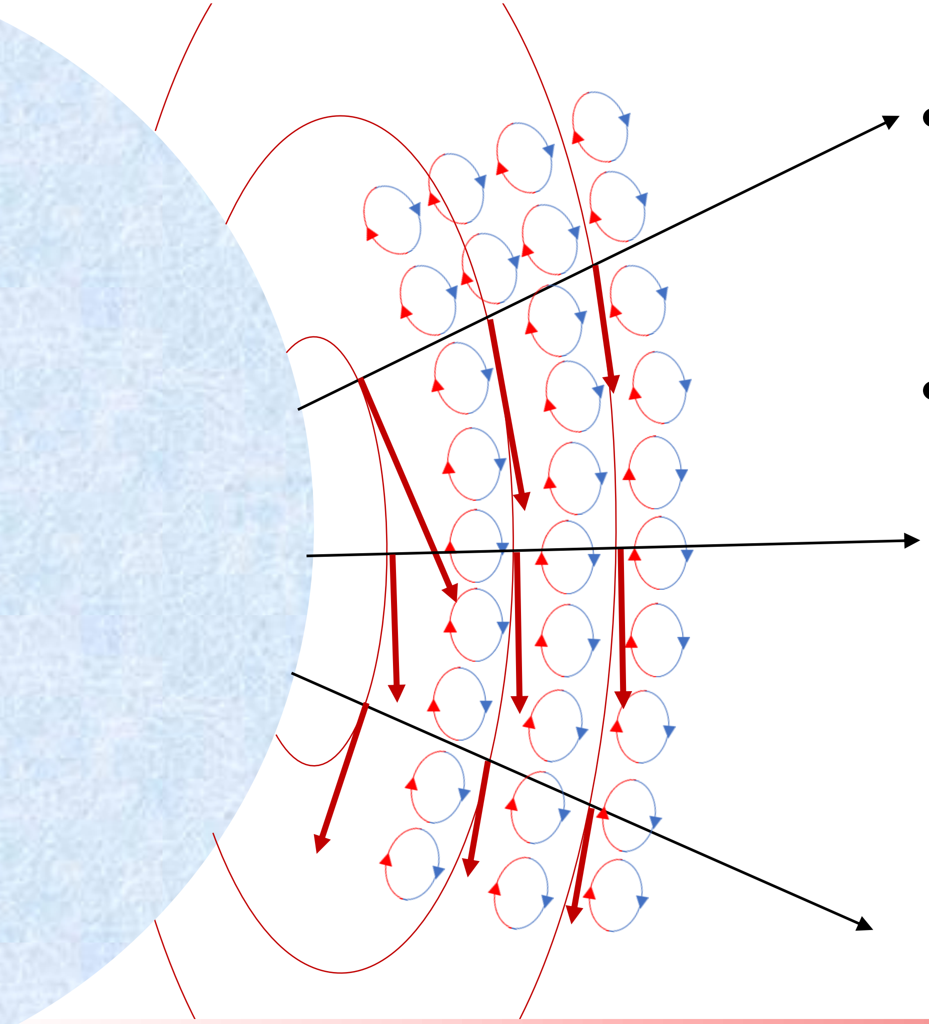

- The polarization pattern of photons at the surface should be quite reduced due to the rapid variation of the magnetic field at the emission
- Strong magnetic fields ($B \gtrsim B_\mathrm{q} = 4.4 \times 10^{13}$ G) can polarize the virtual e^+e^- pairs in the vacuum around the star

Polarization in strong B-fields – QED effects

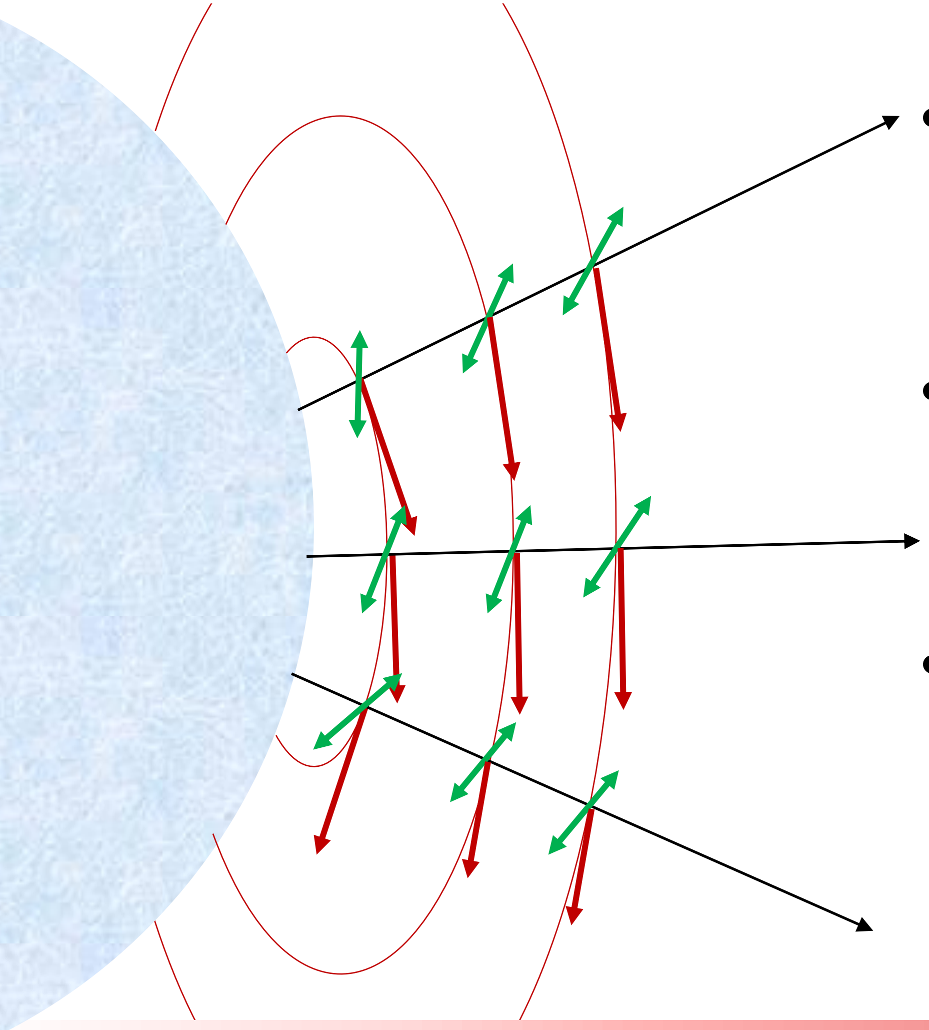

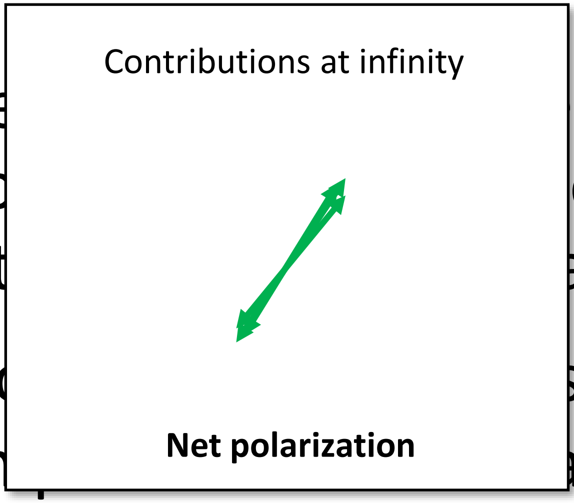

- The rn of photons at the surface sho ed due to the rapid variation of t at the emission
- Str s ($B \gtrsim B_{\mathrm{q}} = 4.4 \times 10^{13}$ G) can al $e^{+}e^{-}$ pairs in the vacuum around the star
- This forces the photon electric field to adiabatically follow the magnetic field, maintaining their original polarization mode up to great distances from the star

Polarization in strong B-fields – QED effects

- The limit within which polarization modes are preserved depends on the star magnetic field strength and on the photon energy

$$\frac{r_\mathrm{a}}{R_\mathrm{NS}} \simeq 4.8 \left(\frac{\hbar\omega}{1\ \mathrm{keV}}\right)^{1/5} \left(\frac{B_\mathrm{p}}{10^{11}\ \mathrm{G}}\right)^{2/5} \left(\frac{R_\mathrm{NS}}{10\ \mathrm{km}}\right)^{1/5}$$

- The observed polarization pattern faithfully traces that at the emission as long as r_a is sufficiently large

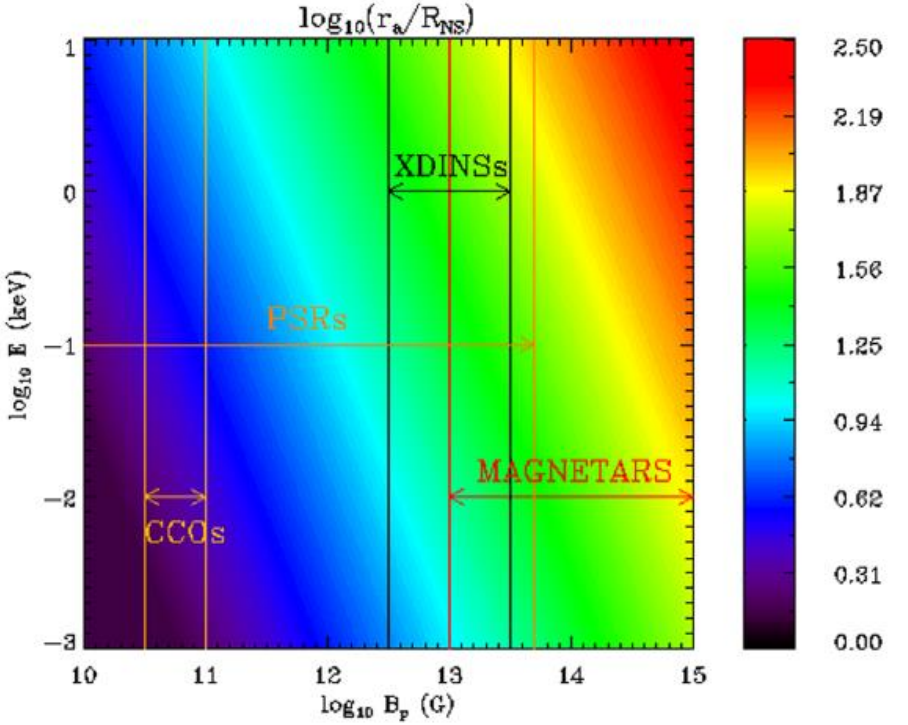

Taverna et al. (2015)

- If QED effects were not present the observed polarization would be extremely low

Polarization in strong B-fields – plasma effects

- Photon polarization state may change in the interactions with matter in strong magnetic fields
- X-mode opacities are normally much suppressed with respect to O-mode ones

Polarization in strong B-fields – plasma effects

- Photon polarization state may change in the interactions with matter in strong magnetic fields
- X-mode opacities are normally much suppressed with respect to O-mode ones
- RCS cross sections:

$$\sigma_{\mathrm{O-O}} = \frac{\pi^2 e^2}{2m_{\mathrm{e}}c}\delta(\omega - \omega_{\mathrm{D}})\cos\vartheta = \frac{1}{3}\sigma_{\mathrm{O-X}}$$

$$\sigma_{\mathrm{X-X}} = \frac{3\pi^2 e^2}{2m_{\mathrm{e}}c}\delta(\omega - \omega_{\mathrm{D}}) = 3\sigma_{\mathrm{X-O}}$$

Surface emission models

- 100%-polarized BB radiation at a constant temperature T over the star surface

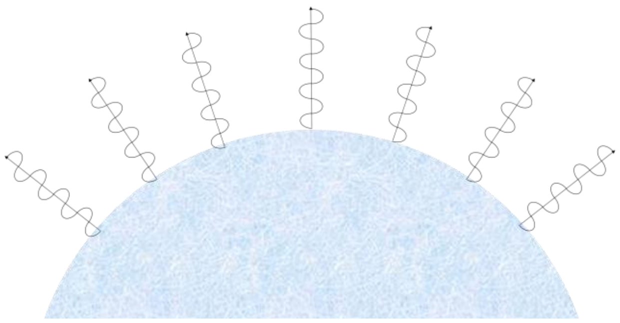

Surface emission models

- 100%-polarized BB radiation at a constant temperature T over the star surface

- Radiation reprocessed in a geometrically-thin optically-thick atmospheric layer (magnetized, pure-H, Suleimanov et al. 2009)

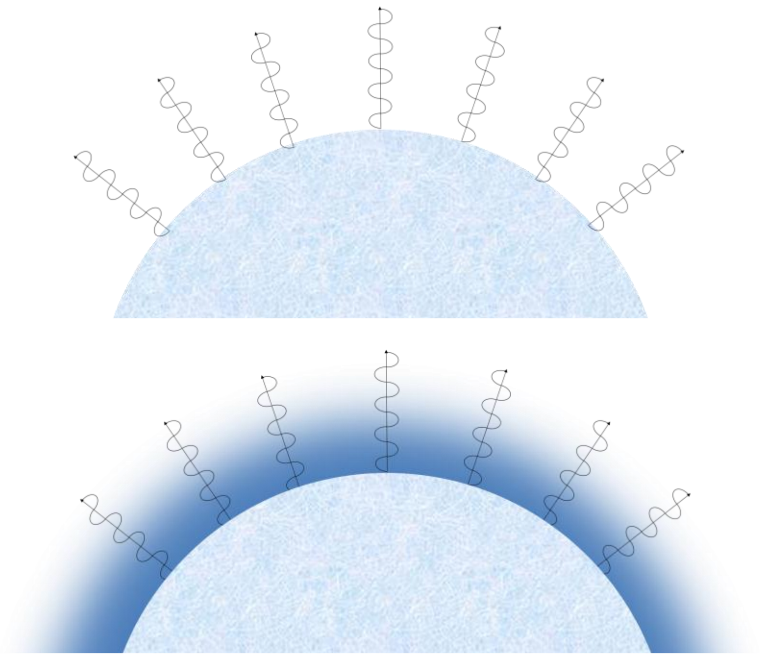

Surface emission models

- 100%-polarized BB radiation at a constant temperature T over the star surface

- Radiation reprocessed in a geometrically-thin optically-thick atmospheric layer (magnetized, pure-H, Suleimanov et al. 2009)

- «Bare», solid surface made by a magnetic condensate formed for sufficiently high B and sufficiently low T (Potekhin et al. 2012)

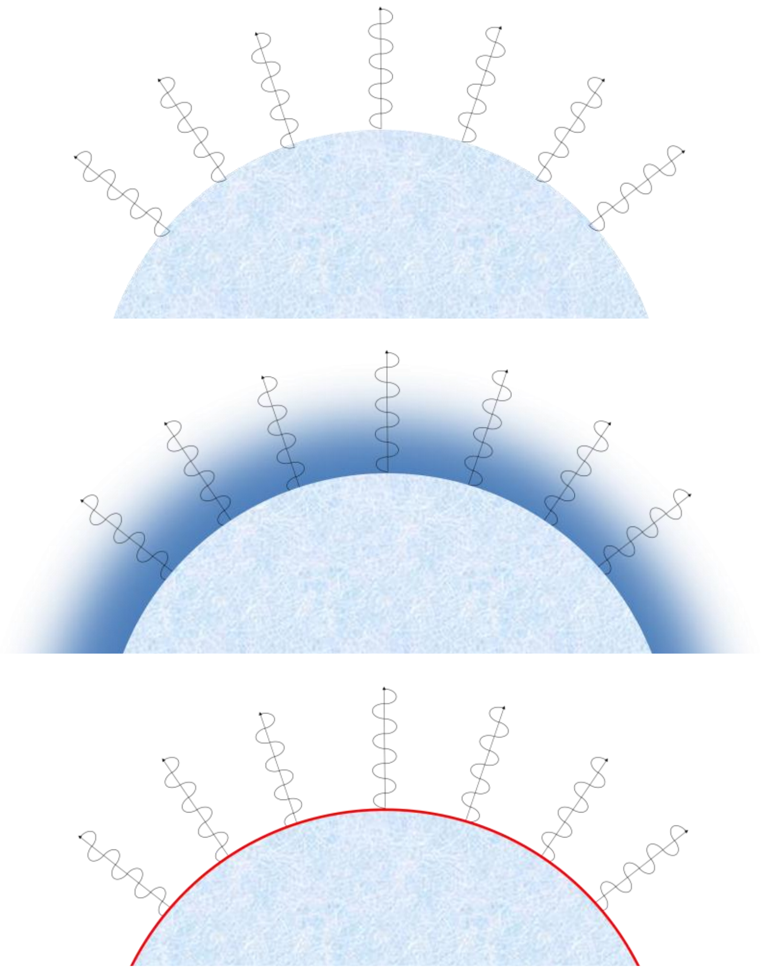

Surface emission models

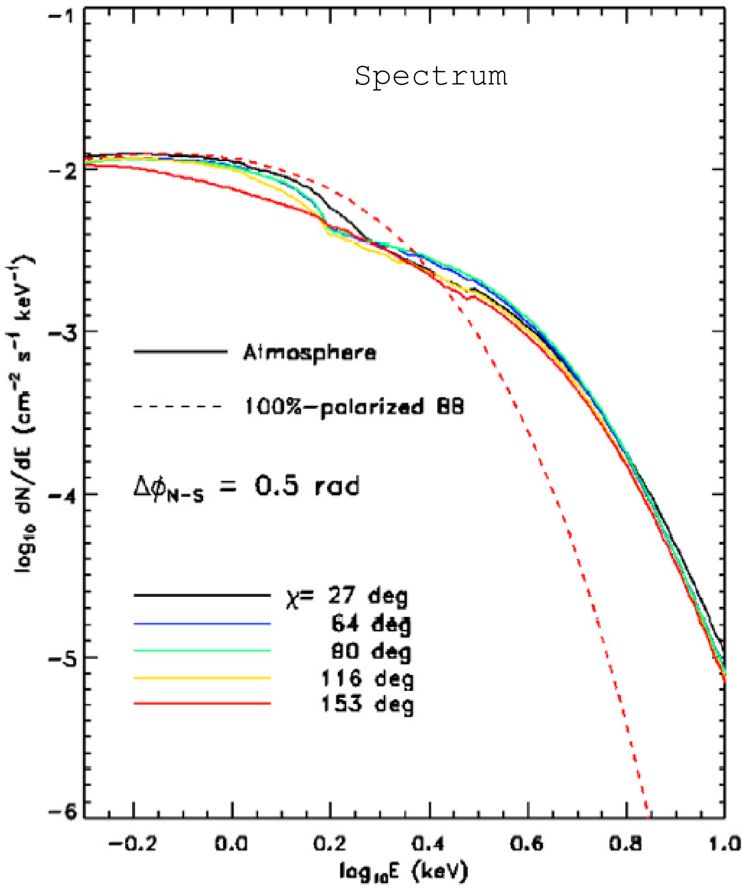

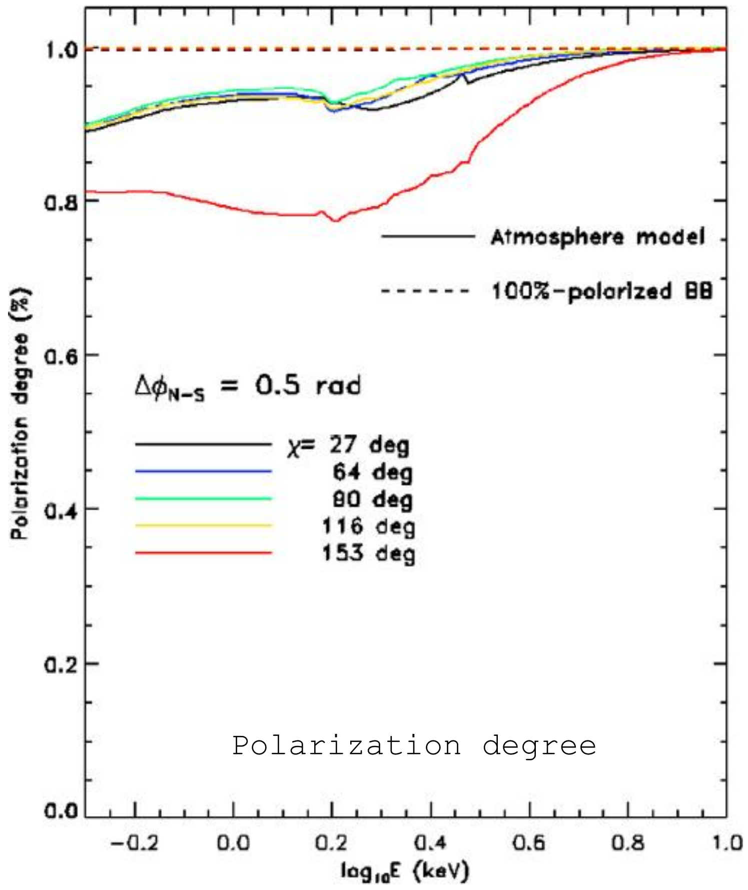

Taverna et al. (2020)

Surface emission models

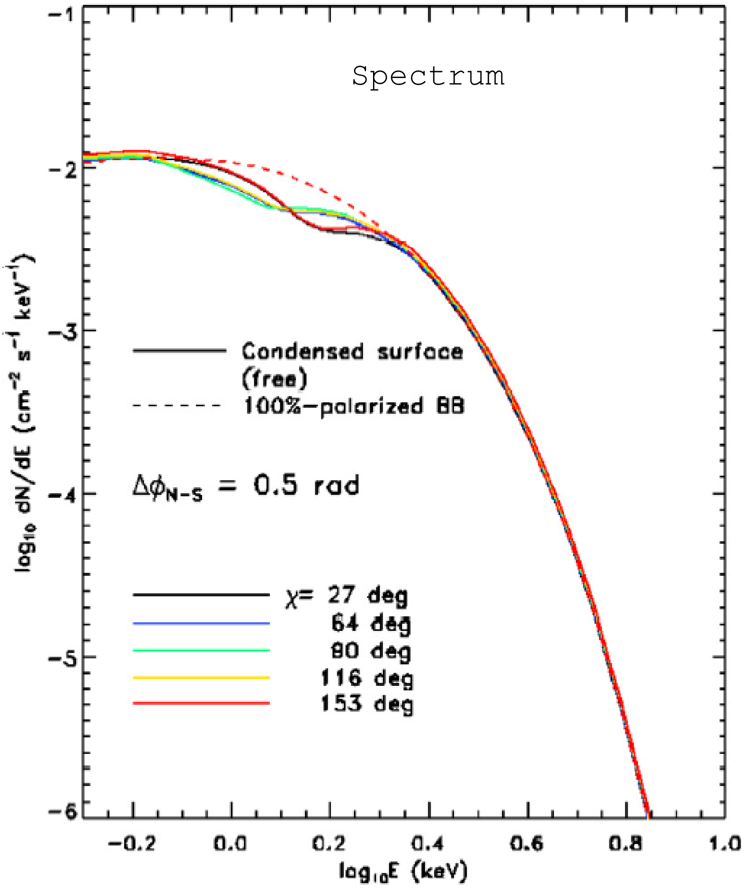

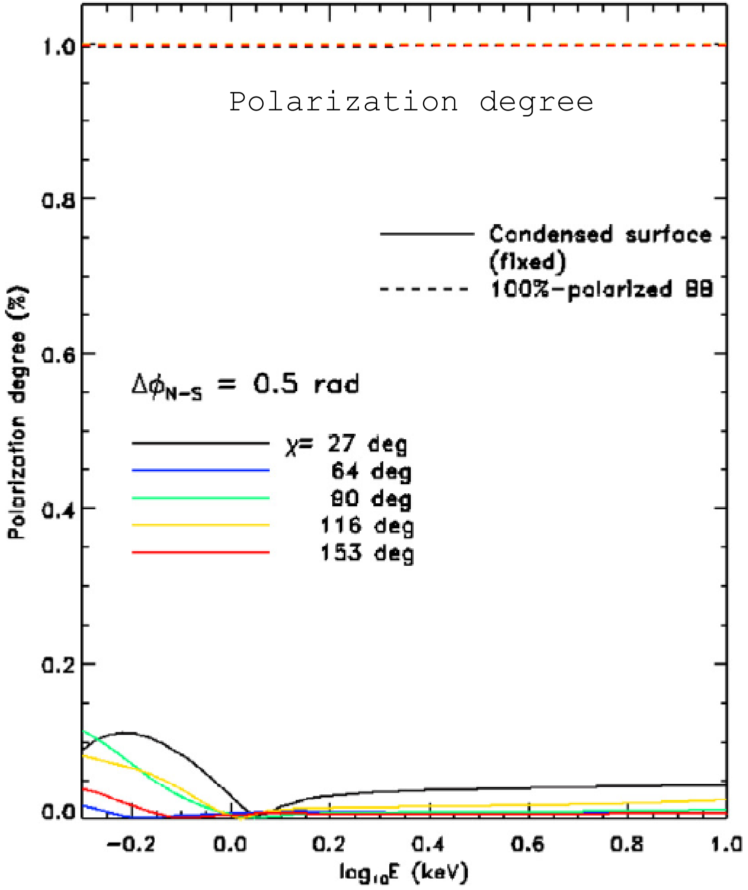

Taverna et al. (2020)

Numerical implementation

- Monte Carlo FORTRAN code (Nobili, Turolla & Zane 2008; Taverna et al. 2014) to reproduce spectra and polarization properties of magnetar persistent radiation collected at infinty

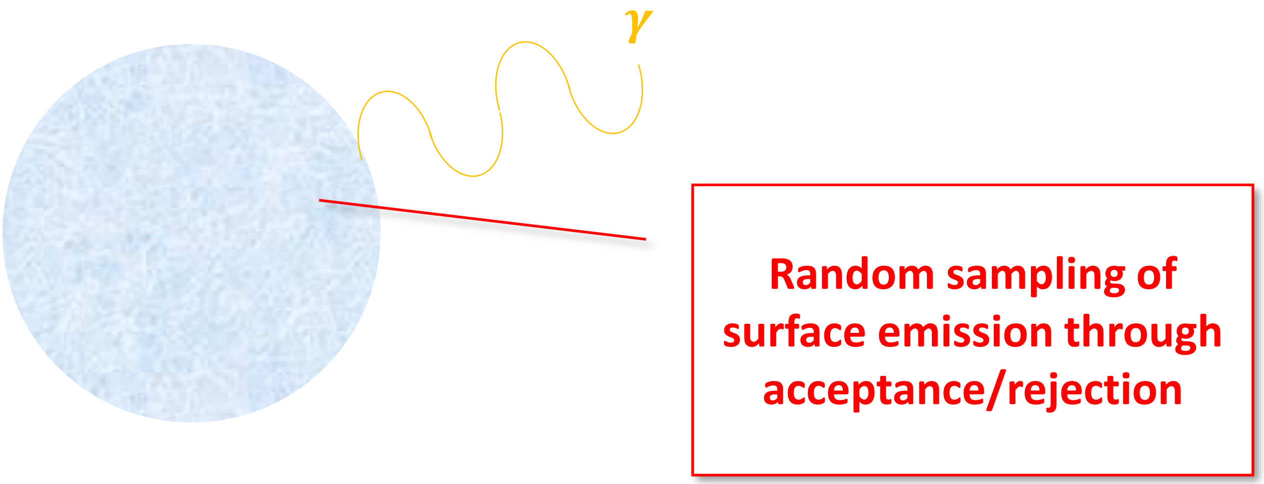

Numerical implementation

- Monte Carlo FORTRAN code (Nobili, Turolla & Zane 2008; Taverna et al. 2014) to reproduce spectra and polarization properties of magnetar persistent radiation collected at infinty

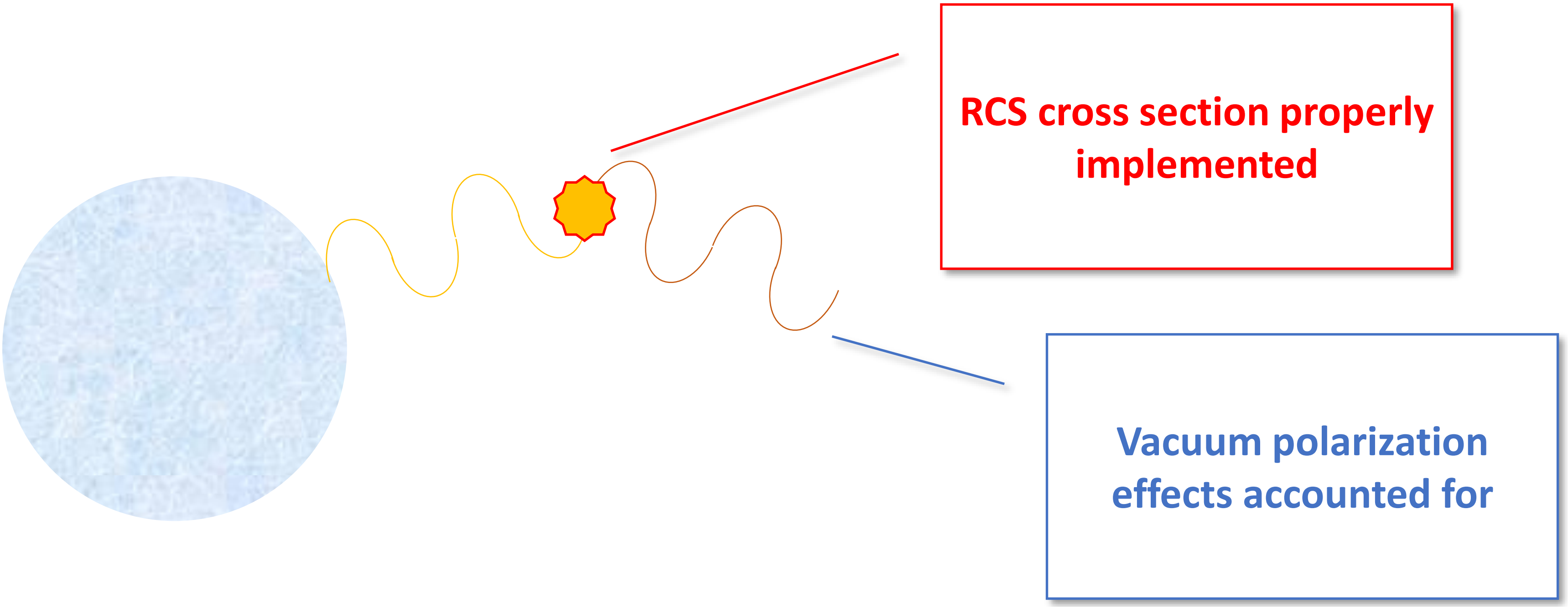

Numerical implementation

- Monte Carlo FORTRAN code (Nobili, Turolla & Zane 2008; Taverna et al. 2014) to reproduce spectra and polarization properties of magnetar persistent radiation collected at infinty

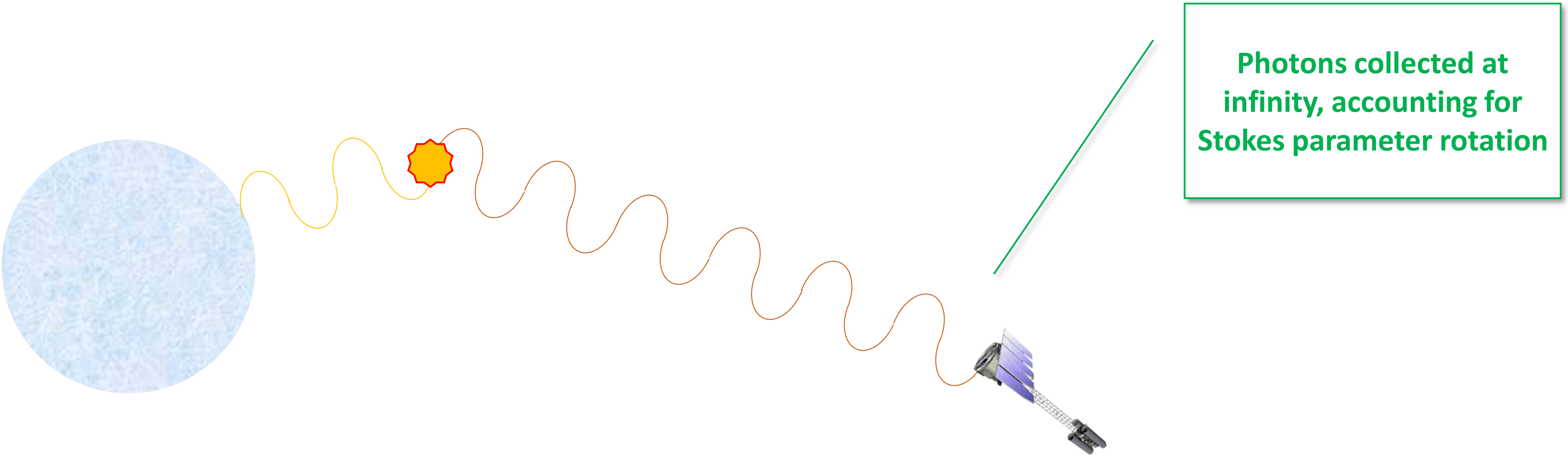

Numerical implementation

- Monte Carlo FORTRAN code (Nobili, Turolla & Zane 2008; Taverna et al. 2014) to reproduce spectra and polarization properties of magnetar persistent radiation collected at infinty
- Specific IDL script to introduce the source geometry

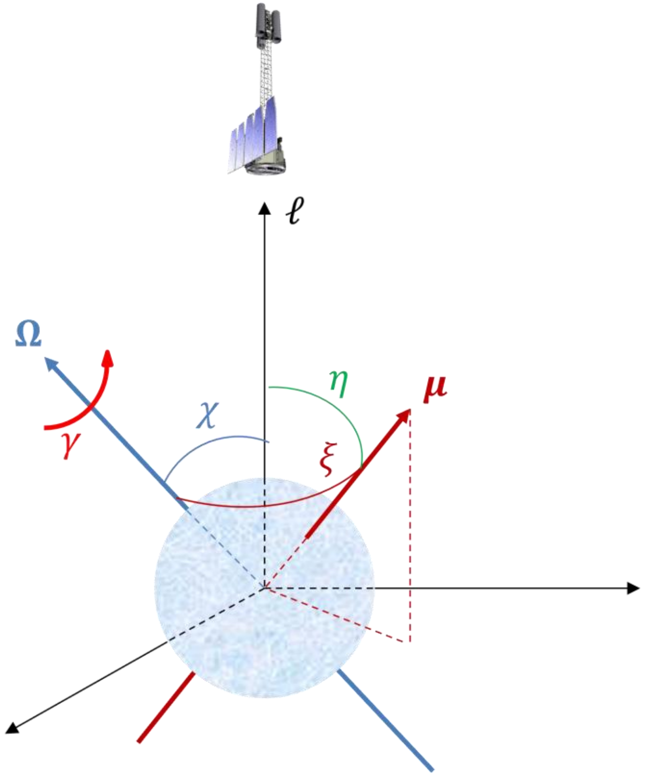

Numerical implementation

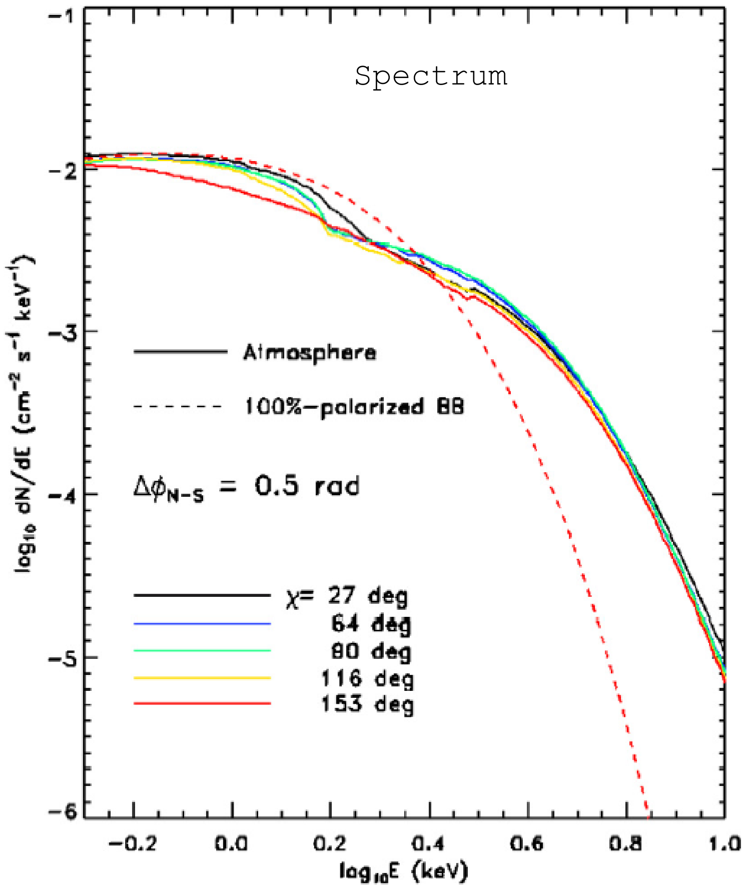

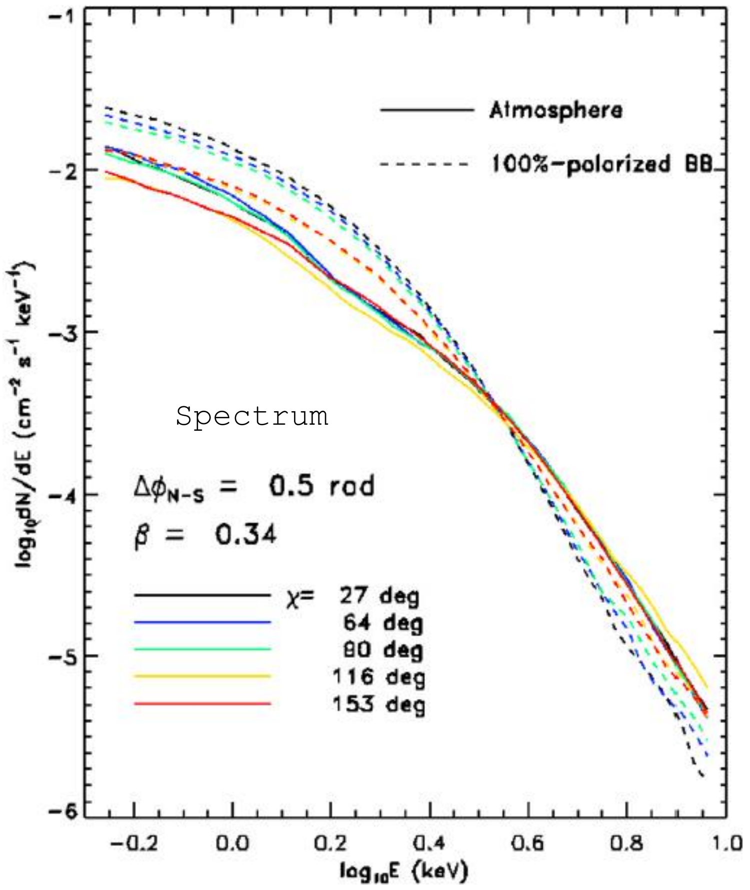

Taverna et al. (2020)

Numerical implementation

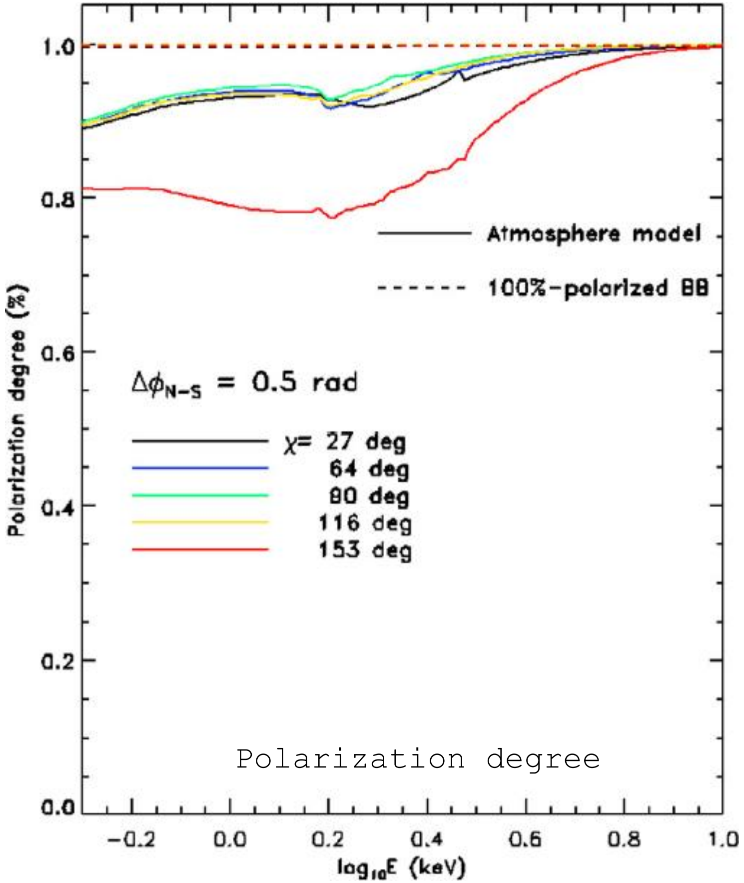

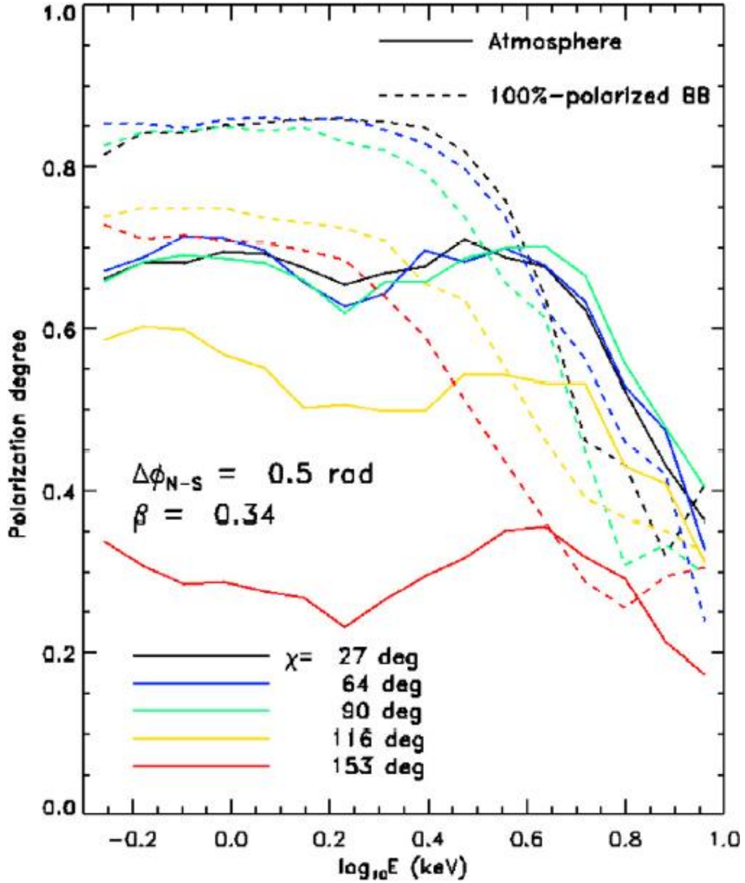

Taverna et al. (2020)

Numerical implementation

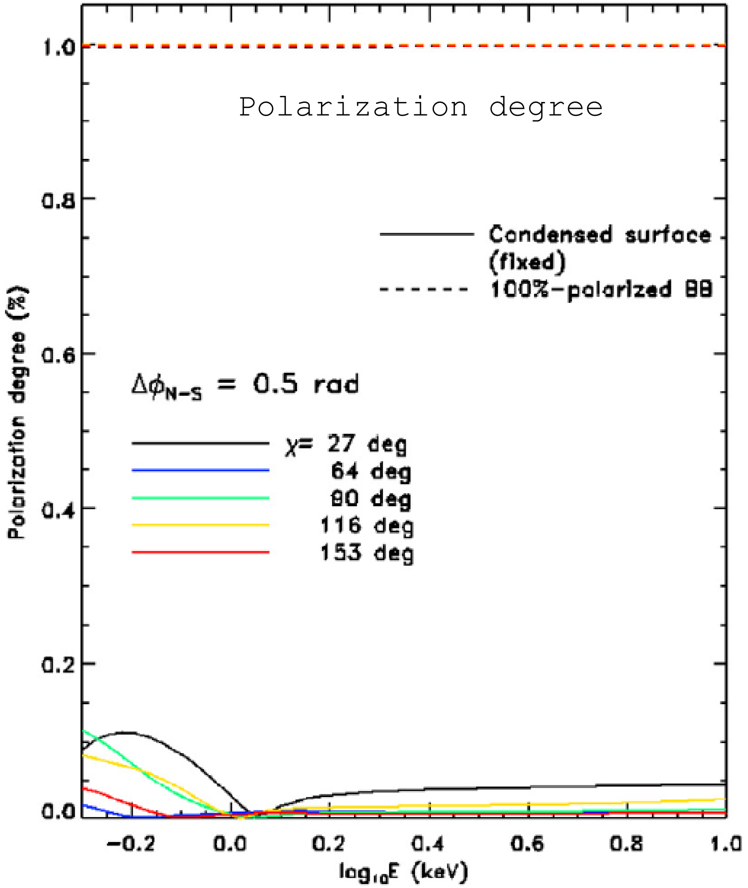

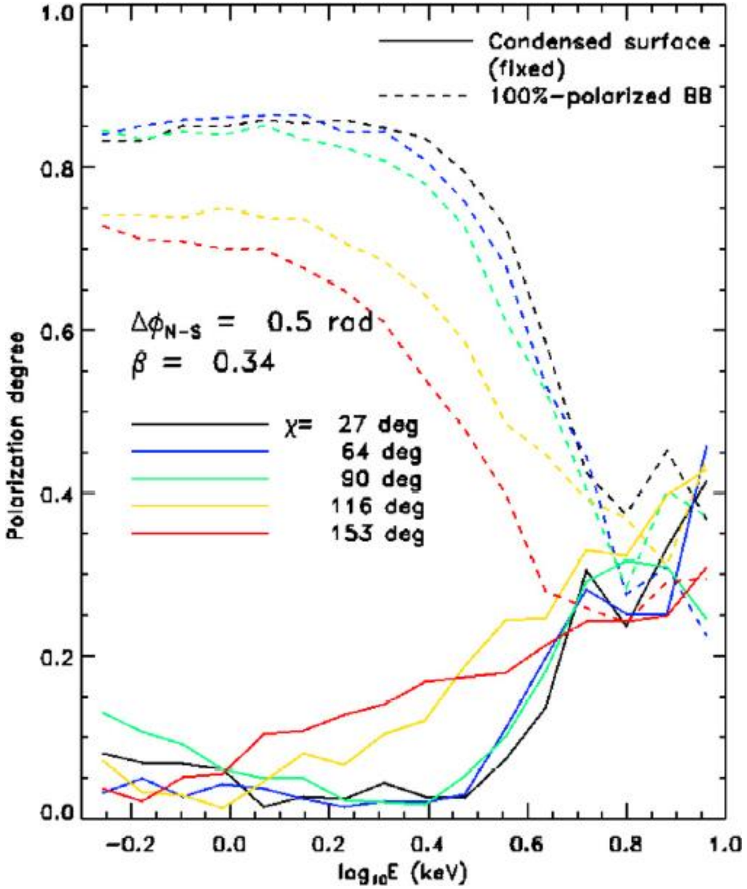

Taverna et al. (2020)

X-ray polarimetry: missions

- $IXPE$ (Imaging X-ray Polarimeter Explorer)
  NASA-SMEX program
  NASA-ASI collaboration
  Expected launch: December 2021

- $eXTP$ (enhanced X-ray Timing Polarimetry)
  Chinese Academy of Science
  CAS-INAF
  Expected launch: 2027

X-ray polarimetry: Gas Pixel Detector

- Photoelectric polarimeters ensure enough sensitivity between $2 - 10\ \mathrm{keV}$

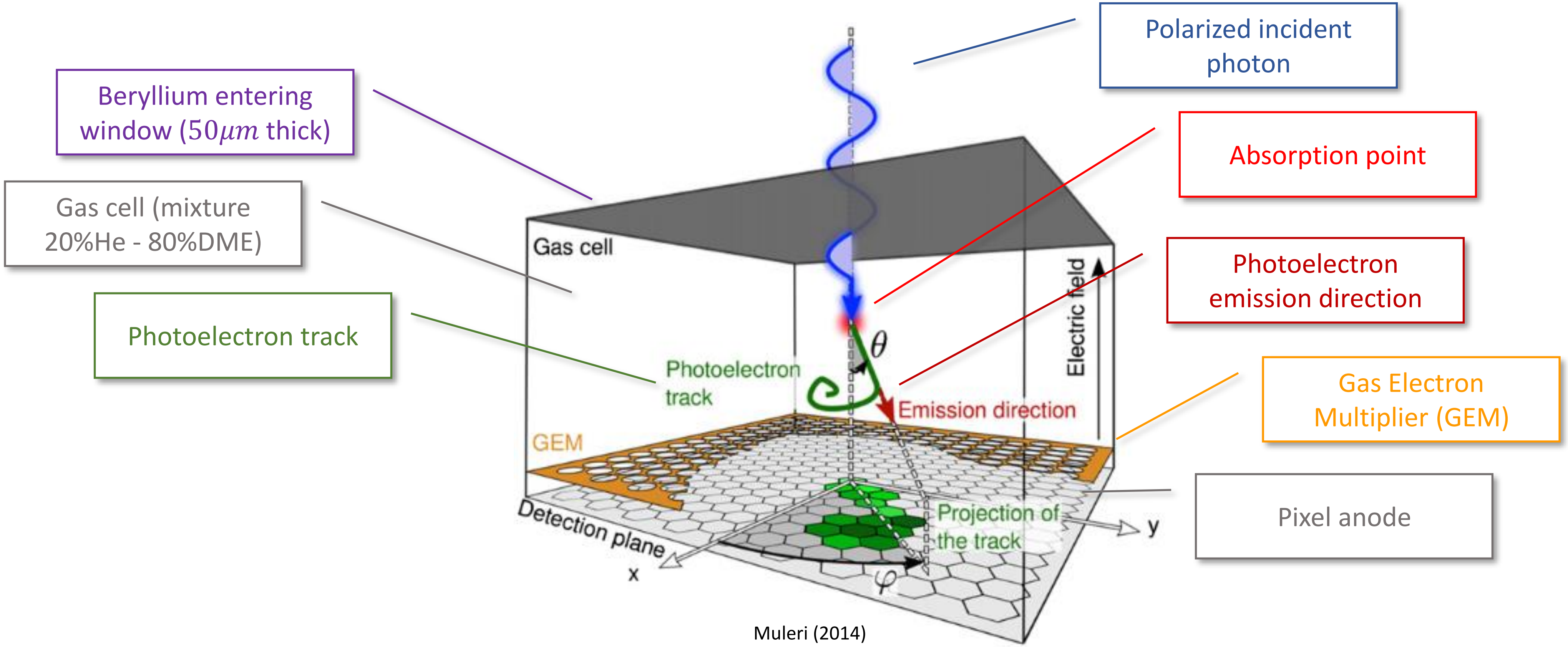

Muleri (2014)

X-ray polarimetry: Gas Pixel Detector

- Photoelectric polarimeters ensure enough sensitivity between $2 - 10\ \mathrm{keV}$
- Photoelectric effect is sensitive to polarization

$$\frac{d\sigma_{Ph}}{d\Omega} = r_0^2 \alpha^4 Z^5 \left(\frac{m_e c^2}{\hbar\omega}\right)^{7/2} \frac{4\sqrt{2}\sin^2\theta\cos^2\varphi}{(1-\beta\cos\theta)^4}$$

Photoelectrons are most probably emitted in the direction of E

φ = photoelectron emission direction – photon E-field angle

X-ray polarimetry: Gas Pixel Detector

- Photoelectric polarimeters ensure enough sensitivity between $2 - 10\ \mathrm{keV}$
- Photoelectric effect is sensitive to polarization

$$\frac{d\sigma_{Ph}}{d\Omega} = r_0^2 \alpha^4 Z^5 \left(\frac{m_e c^2}{k}\right)^{7/2} \frac{4\sqrt{2}\sin^2\theta\cos^2\varphi}{(1-\beta\cos\theta)^4}$$

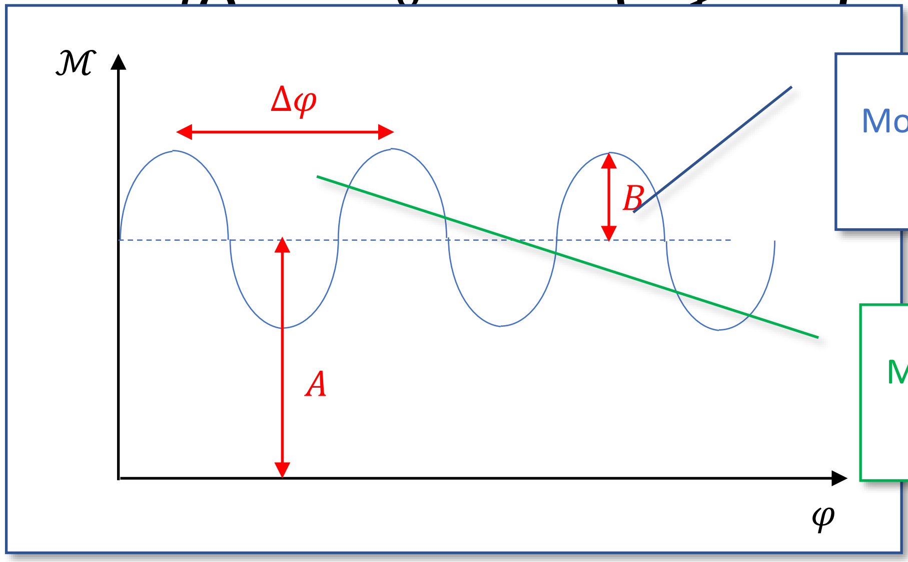

Modulation curve amplitude → polarization degree

Maximum angular position → polarization angle

Simulated measurements

- Archive of theoretical, phase-resolved models for:
  - different values of χ, ξ, $\Delta\phi_{\mathrm{N-S}}$, β
  - different emission models
  - QED-ON and QED-OFF

Simulated measurements

- Archive of theoretical, phase-resolved models for:
  - different values of χ, ξ, $\Delta\phi_{\mathrm{N-S}}$, β
  - different emission models
  - QED-ON and QED-OFF
- Spectro-polarimetry simulation measurement for one specific (blind) set of input parameters (source 1RXS J170849.0-400910, $t_{\mathrm{exp}} = 1\ \mathrm{Ms}$)

Simulated measurements

- Archive of theoretical, phase-resolved models for:
  - different values of χ, ξ, $\Delta\phi_{\mathrm{N-S}}$, β
  - different emission models
  - QED-ON and QED-OFF
- Spectro-polarimetry simulation measurement for one specific (blind) set of input parameters (source 1RXS J170849.0-400910, $t_{\mathrm{exp}} = 1\ \mathrm{Ms}$)
- Fit of the mock-data with the whole archive

Timing analysis

- Data analysis through the python tool HENDRICS (Bachetti, 2018)

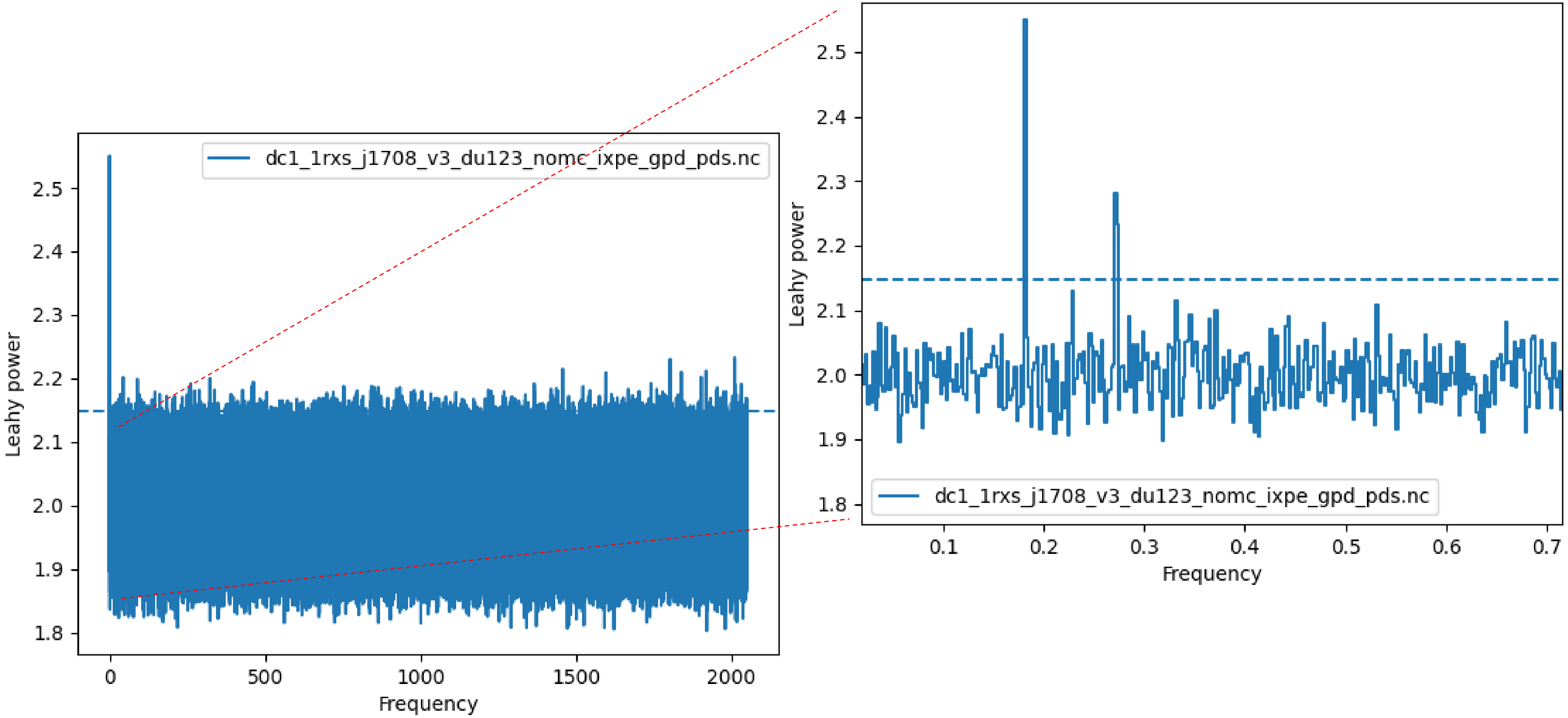

Timing analysis

- Data analysis through the python tool HENDRICS (Bachetti, 2018)
- Z^2-search of the period and period derivative of the source

	$\boldsymbol{P}$ **(s)**	$\dot{\boldsymbol{P}}$ **(s/s)**
mock data	11.010	2.1×10^{-11}
Dib & Kaspi (2014)	11.005	2.0×10^{-11}

Timing analysis

- Data analysis through the python tool HENDRICS (Bachetti, 2018)
- Z^2-search of the period and period derivative of the source
- Data have been binned into 9 phase bins

Spectro-Polarimetric analysis

- Phase-dependent fit of the mock data energy integrated between $2-8\ \mathrm{keV}$

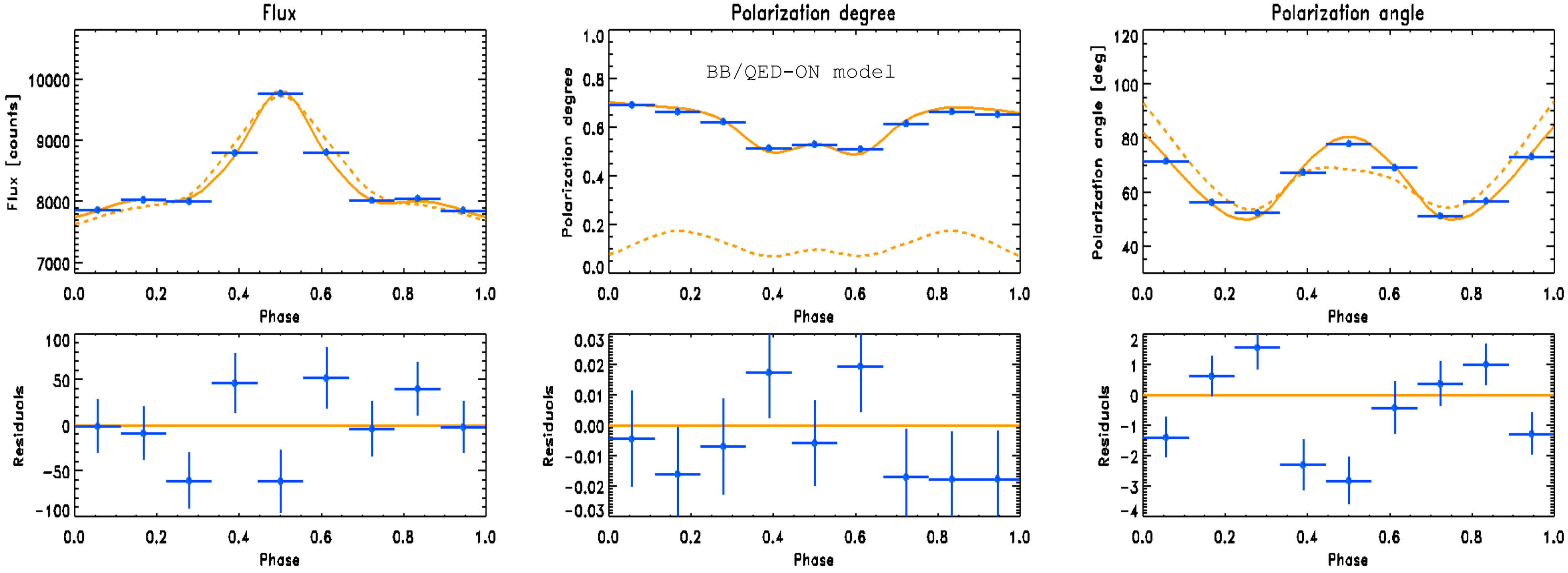

Spectro-Polarimetric analysis

- Phase-dependent fit of the mock data energy integrated between $2-8\ \mathrm{keV}$

	BB QED-ON (2-8 keV)	BB QED-OFF (2-8 keV)	free QED-ON (2-8)	free QED-OFF (2-8)
chi	82.68 ± 0.71	86.45 ± 0.54	61.70 ± 0.66	92.49 ± 0.34
xi	55.60 ± 0.41	39.40 ± 0.41	58.59 ± 0.09	38.25 ± 0.29
Dphi	0.442 ± 0.011	0.310 ± 0.000	0.574 ± 0.010	0.310 ± 0.000
beta	0.238 ± 0.012	0.573 ± 0.009	0.690 ± 0.010	0.690 ± 0.000
log(N)	1.560 ± 0.003	1.497 ± 0.001	1.379 ± 0.001	1.397 ± 0.001
chisq	2.619	449.502	381.403	634.216

***   ***

	atmo QED-ON (2-8 keV)	atmo QED-OFF (2-8 keV)	fix QED-ON (2-8)	fix QED-OFF (2-8)
chi	86.75 ± 0.41	90.90 ± 0.20	81.19 ± 0.59	117.17 ± 1.84
xi	48.32 ± 0.27	42.55 ± 0.25	44.60 ± 0.32	9.39 ± 0.43
Dphi	0.310 ± 0.000	0.513 ± 0.005	0.310 ± 0.000	1.390 ± 0.000
beta	0.685 ± 0.035	0.690 ± 0.000	0.685 ± 0.011	0.301 ± 0.009
log(N)	1.227 ± 0.000	1.214 ± 0.001	1.372 ± 0.001	1.264 ± 0.006
chisq	32.909	491.034	390.859	357.375

Spectro-Polarimetric analysis

- Phase-dependent fit of the mock data energy integrated between $2-8\ \mathrm{keV}$

	BB QED-ON (2-8 keV)	BB QED-OFF (2-8 keV)		free QED-ON (2-8)	free QED-OFF (2-8)
chi	82.68 ± 0.71	86.45 ± 0.54	chi	61.70 ± 0.66	92.49 ± 0.34
xi	55.60 ± 0.41	39.40 ± 0.41	xi	58.59 ± 0.09	38.25 ± 0.29
Dphi	0.442 ± 0.011	0.310 ± 0.000	Dphi	0.574 ± 0.010	0.310 ± 0.000
beta	0.238 ± 0.012	0.573 ± 0.009	beta	0.690 ± 0.010	0.690 ± 0.000
log(N)	1.560 ± 0.003	1.497 ± 0.001	log(N)	1.379 ± 0.001	1.397 ± 0.001
chisq	2.619	449.502	chisq	381.403	634.216

*** ***

	atmo QED-ON (2-8 keV)	atmo QED-OFF (2-8 keV)		fix QED-ON (2-8)	fix QED-OFF (2-8)
chi	86.75 ± 0.41	90.90 ± 0.20	chi	81.19 ± 0.59	117.17 ± 1.84
xi	48.32 ± 0.27	42.55 ± 0.25	xi	44.60 ± 0.32	9.39 ± 0.43
Dphi	0.310 ± 0.000	0.513 ± 0.005	Dphi	0.310 ± 0.000	1.390 ± 0.000
beta	0.685 ± 0.035	0.690 ± 0.000	beta	0.685 ± 0.011	0.301 ± 0.009
log(N)	1.227 ± 0.000	1.214 ± 0.001	log(N)	1.372 ± 0.001	1.264 ± 0.006
chisq	32.909	491.034	chisq	390.859	357.375

Spectro-Polarimetric analysis

- Phase-dependent fit of the mock data energy integrated between $2 - 8\ \mathrm{keV}$
- Spectral analysis through the Heasoft tool XSPEC (Arnoud, 1996)

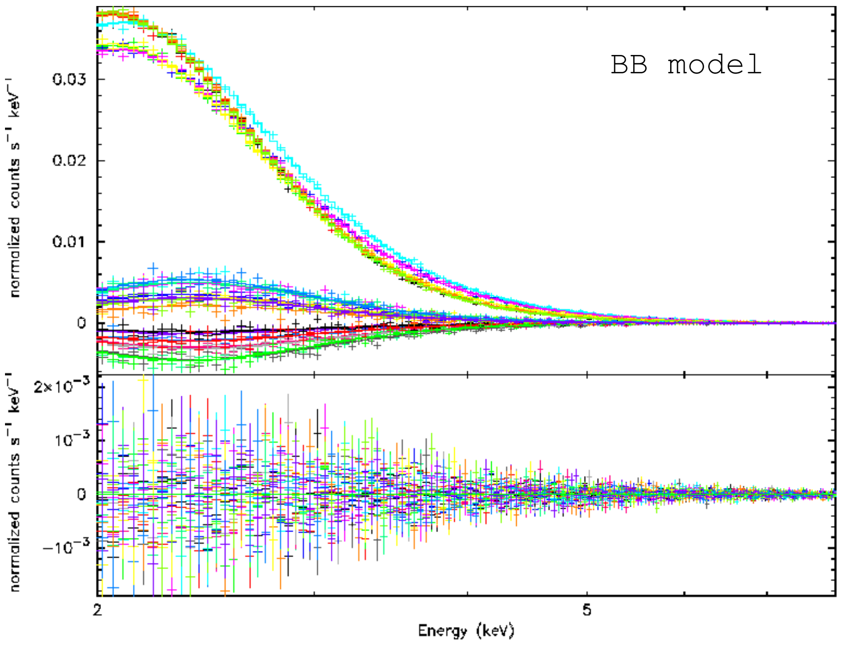

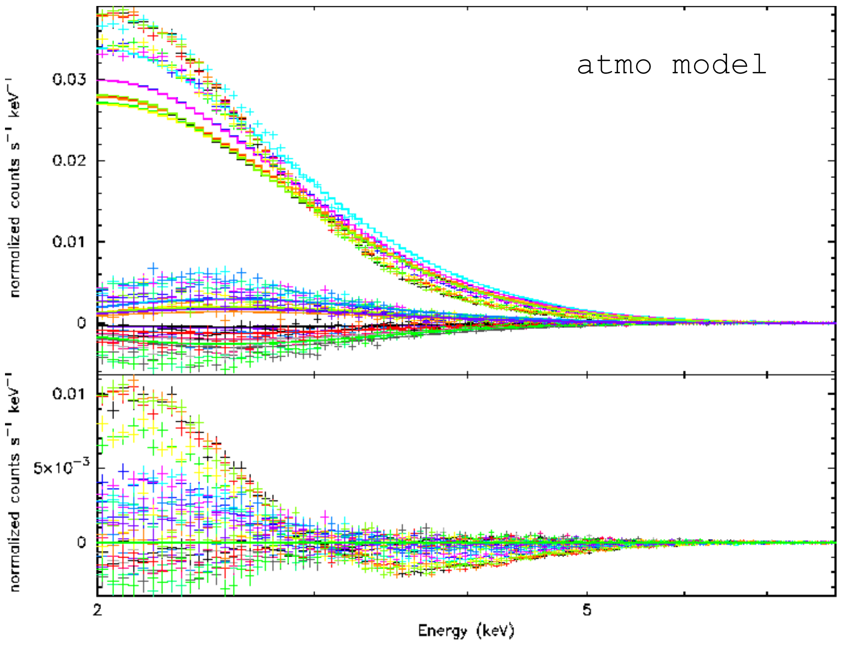

Spectro-Polarimetric analysis

- Phase-dependent fit of the mock data energy integrated between $2-8\ \mathrm{keV}$
- Spectral analysis through the Heasoft tool XSPEC (Arnoud, 1996)

```
BB QED-ON (2-8 keV)          BB QED-OFF (2-8 keV)       free QED-ON (2-8)                 free QED-OFF (2-8)

 chi      93.14 (-1.07,+1.08)  89.91 (-0.13,+0.15)        chi     122.16 (-0.39,+0.55)    75.01 (-0.06,+0.11)
  xi      36.50 (-2.06,+2.88)  48.40 (-0.95,+0.60)         xi      56.32 (-0.70,+0.43)    58.41 (-0.29,+0.23)
Dphi      0.363 (-0.020,+0.019) 0.408 (-0.003,+0.003)    Dphi      0.422 (-0.004,+0.003)  0.464 (-0.002,+0.002)
beta      0.409 (-0.006,+0.006) 0.362 (-0.003,+0.002)    beta      0.340 (-0.003,+0.002)  0.438 (-0.002,+0.001)
nH(e22)   1.250 (-0.023,+0.024) 1.330 (-0.013,+0.020)    nH(e22)   1.296 (-0.015,+0.013)  1.025 (-0.015,+0.013)

chisq         1.011               1.160                  chisq         1.702                 1.798

***                                                      ***

atmo QED-ON (2-8 keV)        atmo QED-OFF (2-8 keV)     fix QED-ON (2-8)                  fix QED-OFF (2-8)

 chi      14.97 (-0.08,+0.06)  39.31 (-0.44,+0.46)        chi     104.95 (-1.11,+0.10)    78.44 (-0.93,+0.54)
  xi       0.10 (-0.10,+0.01)  50.07 (-0.11,+0.11)         xi      76.41 (-0.08,+0.08)    53.73 (-1.01,+0.36)
Dphi      0.300 (-0.300,+0.000) 0.300 (-0.300,+0.000)    Dphi      0.829 (-0.015,+0.006)  0.500 (-0.001,+0.001)
beta      0.218 (-0.004,+0.005) 0.200 (-0.200,+0.000)    beta      0.203 (-0.002,+0.002)  0.354 (-0.001,+0.001)
nH(e22)   5e-18 (-0.000,+0.822) 5e-17 (-0.000,+0.822)    nH(e22)   0.822 (-0.014,+0.015)  1.326 (-0.017,+0.013)

chisq         5.112               5.912                  chisq         1.488                 1.875
```

Spectro-Polarimetric analysis

- Phase-dependent fit of the mock data energy integrated between $2-8\ \mathrm{keV}$
- Spectral analysis through the Heasoft t

	BB QED-ON (2-8 keV)	BB QED-OFF (2-8 keV)	f	-8)
chi	93.14 (-1.07,+1.08)	89.91 (-0.13,+0.15)		.11)
xi	36.50 (-2.06,+2.88)	48.40 (-0.95,+0.60)		.23)
Dphi	0.363 (-0.020,+0.019)	0.408 (-0.003,+0.003)	D	.002)
beta	0.409 (-0.006,+0.006)	0.362 (-0.003,+0.002)	b	.001)
nH(e22)	1.250 (-0.023,+0.024)	1.330 (-0.013,+0.020)	n	.013)
chisq	1.011	1.160	c	

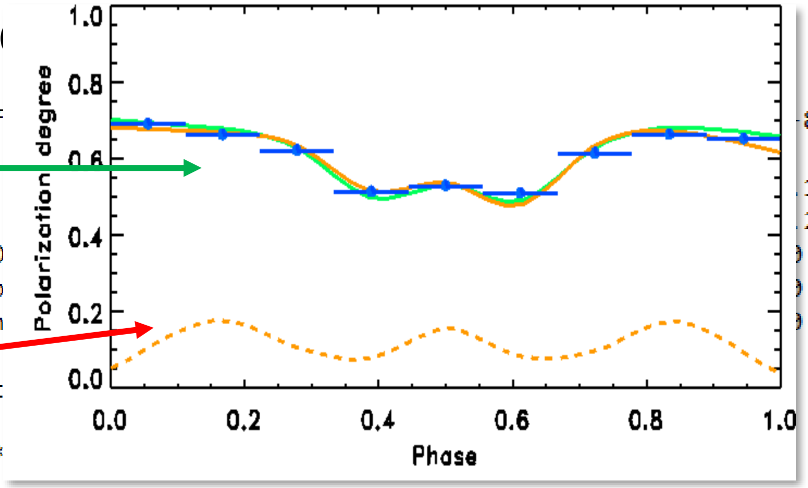

*** *

	atmo QED-ON (2-8 keV)	atmo QED-OFF (2-8 keV)	fix QED-ON (2-8)	fix QED-OFF (2-8)
chi	14.97 (-0.08,+0.06)	39.31 (-0.44,+0.46)	104.95 (-1.11,+0.10)	78.44 (-0.93,+0.54)
xi	0.10 (-0.10,+0.01)	50.07 (-0.11,+0.11)	76.41 (-0.08,+0.08)	53.73 (-1.01,+0.36)
Dphi	0.300 (-0.300,+0.000)	0.300 (-0.300,+0.000)	0.829 (-0.015,+0.006)	0.500 (-0.001,+0.001)
beta	0.218 (-0.004,+0.005)	0.200 (-0.200,+0.000)	0.203 (-0.002,+0.002)	0.354 (-0.001,+0.001)
nH(e22)	5e-18 (-0.000,+0.822)	5e-17 (-0.000,+0.822)	0.822 (-0.014,+0.015)	1.326 (-0.017,+0.013)
chisq	5.112	5.912	1.488	1.875

Data analysis - Summary

Phase dependent analysis (2-8 keV)

	Fit param	1-σ error
χ	$82.68°$	$0.71°$
ξ	$55.60°$	$0.41°$
$\Delta\phi$	0.442 rad	0.011 rad
β	0.238	0.012
χ^2_{red}	2.619	

Spectral analysis

	Fit param	1-σ error
χ	$93.14°$	$1.08°$
ξ	$36.50°$	$2.47°$
$\Delta\phi$	0.363 rad	0.020 rad
β	0.409	0.006
χ^2_{red}	1.011	

Data analysis - Summary

Phase dependent analysis (2-8 keV)

	Fit param	1-σ error
χ	82.68°	0.71°
ξ	55.60°	0.41°
$\Delta\phi$	0.442 rad	0.011 rad
β	0.238	0.012
χ^2_{red}	2.619	

Spectral analysis

	Fit param	1-σ error
χ	93.14°	1.08°
ξ	36.50°	2.47°
$\Delta\phi$	0.363 rad	0.020 rad
β	0.409	0.006

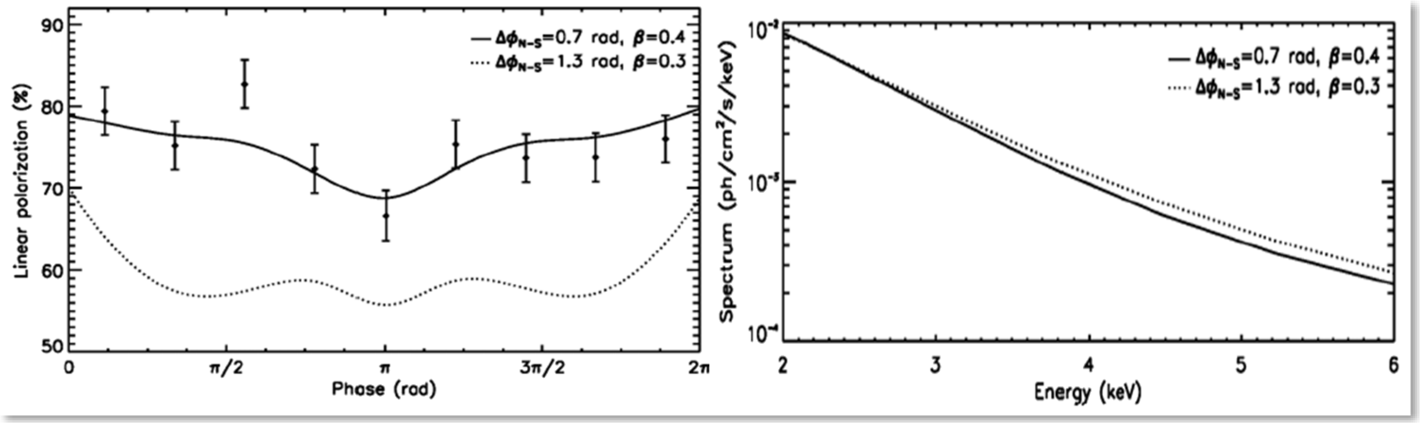

Taverna et al. (2014)

Data analysis - Summary

Phase dependent analysis (2-8 keV)

	Fit param	1-σ error
χ	$82.68°$	$0.71°$
ξ	$55.60°$	$0.41°$
$\Delta\phi$	0.442 rad	0.011 rad
[illegible]	[illegible]	[illegible]12
$\chi^2_{\rm red}$	2.619	

PA and PD phase-dependent behaviors are sensitive to χ and ξ

Spectral analysis

	Fit param	1-σ error
χ	[illegible]	[illegible]
ξ	[illegible]	[illegible]
$\Delta\phi$	0.363 rad	0.020 rad
β	0.409	0.006
$\chi^2_{\rm red}$	1.011	

Spectra (PL tails) are sensitive to $\Delta\phi$ and β

Data analysis - Summary

Phase dependent analysis (2-8 keV)

	Fit param	1-σ error
χ	82.68°	0.71°
ξ	55.60°	0.41°
$\Delta\phi$	0.442 rad	0.011 rad
		12
χ^2_{red}	2.619	

PA and PD phase-dependent behaviors are sensitive to χ and ξ

Spectral analysis

	Fit param	1-σ error
χ		
ξ		
$\Delta\phi$	0.363 rad	0.020 rad
β	0.409	0.006
χ^2_{red}	1.011	

Spectra (PL tails) are sensitive to $\Delta\phi$ and β

- Original mock data input parameters:

$$\text{emission model:} \rightarrow \text{ 100\% polarized BB}$$
$$\chi = 85° \; - \; \xi = 55° \; - \; \Delta\phi_{\mathrm{N-S}} = 0.35 \text{ rad} \; - \; \beta = 0.39$$

Spectral fitting of XMM-Newton data

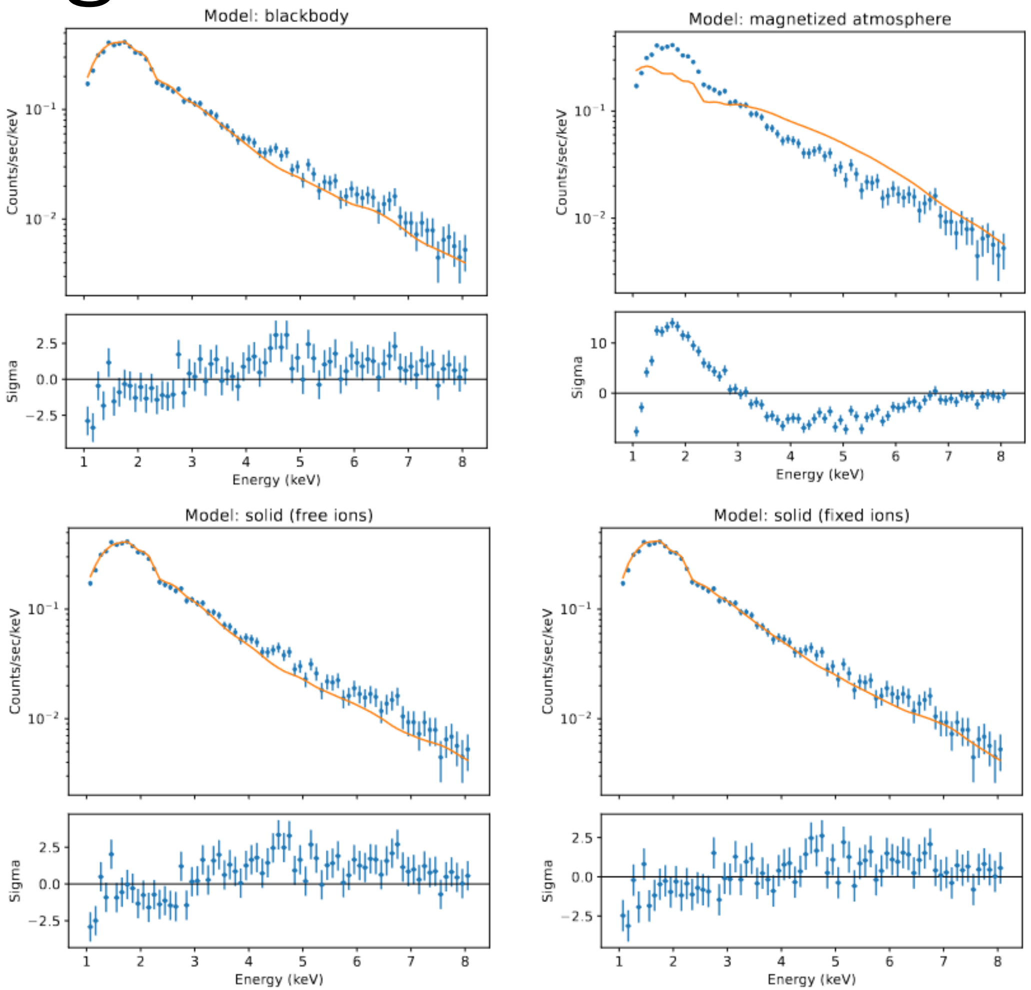

Krawczynski et al. (submitted)

Spectral fitting of XMM-Newton data

XMM-Newton observation (Aug 28-29, 2003, 44.7 ks)

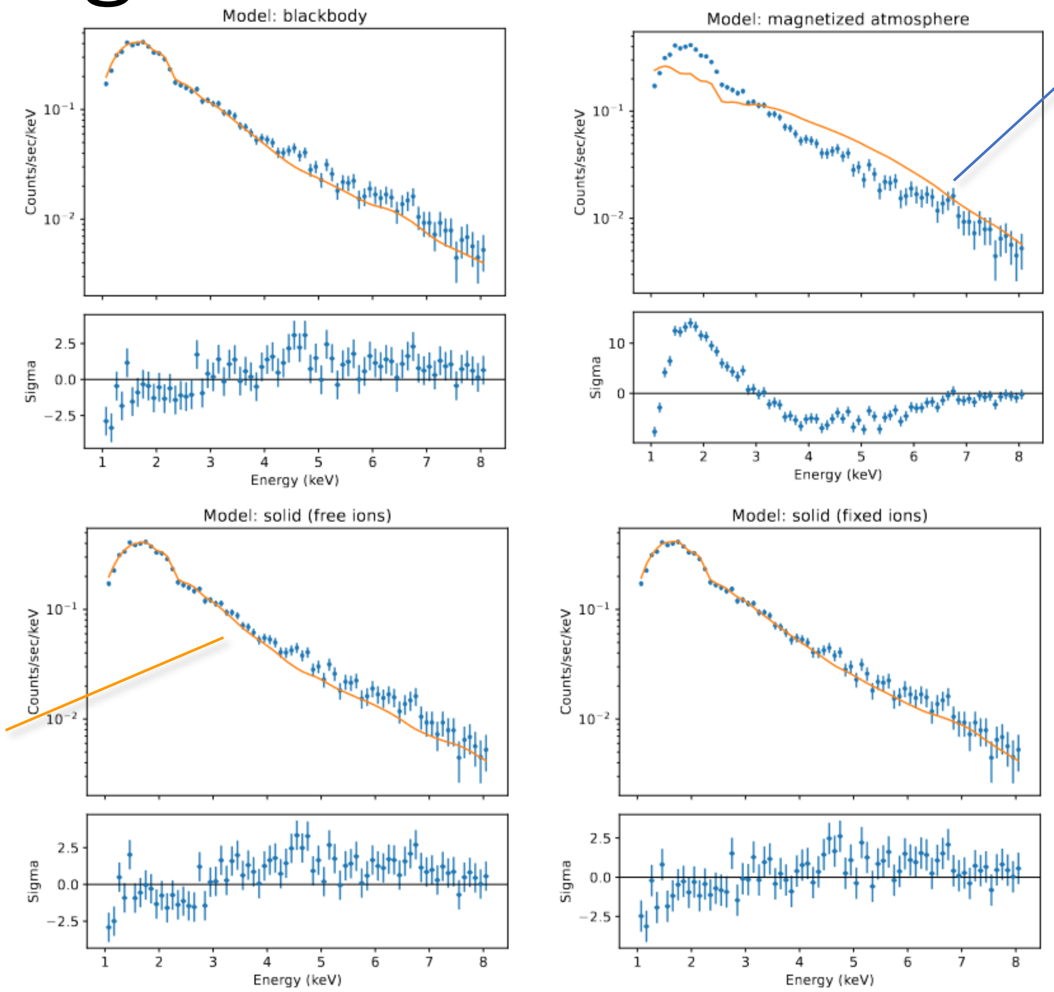

Best fitting curve

Krawczynski et al. (submitted)

Conclusions

- Both phase-dependent and spectral analyses are necessary to completely determine the viewing geometry and the magnetospheric configuration
- Phase-dependent analysis will allow to test observationally QED vacuum polarization effects (to which spectral fits seem to be quite unsensitive)
- X-ray polarimetry is crucial to determine the surface emission models, removing spectral degeneracies